

## Accepted Manuscript

Tectonic evolution and copper-gold metallogensis of the Papua New Guinea and Solomon Islands region

Robert J. Holm, Simon Tapster, Hielke A. Jelsma, Gideon Rosenbaum, Darren F. Mark

PII: S0169-1368(17)30778-3

DOI: <https://doi.org/10.1016/j.oregeorev.2018.11.007>

Reference: OREGEO 2734

To appear in: *Ore Geology Reviews*

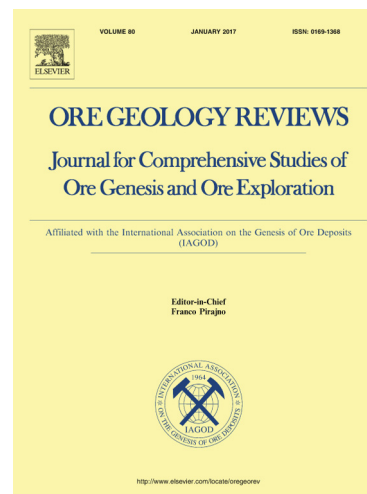
Received Date: 14 October 2017

Revised Date: 4 November 2018

Accepted Date: 8 November 2018

Please cite this article as: R.J. Holm, S. Tapster, H.A. Jelsma, G. Rosenbaum, D.F. Mark, Tectonic evolution and copper-gold metallogensis of the Papua New Guinea and Solomon Islands region, *Ore Geology Reviews* (2018), doi: <https://doi.org/10.1016/j.oregeorev.2018.11.007>

This is a PDF file of an unedited manuscript that has been accepted for publication. As a service to our customers we are providing this early version of the manuscript. The manuscript will undergo copyediting, typesetting, and review of the resulting proof before it is published in its final form. Please note that during the production process errors may be discovered which could affect the content, and all legal disclaimers that apply to the journal pertain.



1           **Tectonic evolution and copper-gold metallogensis of the Papua New**  
2   **Guinea and Solomon Islands region**

3  
4 Robert J. Holm<sup>1,2</sup>, Simon Tapster<sup>3,4</sup>, Hielke A. Jelsma<sup>5</sup>, Gideon Rosenbaum<sup>6</sup>, Darren F.  
5 Mark<sup>7,8</sup>

6  
7 <sup>1</sup>Frogtech Geoscience, 2 King Street, Deakin West, ACT 2600, Australia

8 <sup>2</sup>Economic Geology Research Centre (EGRU), James Cook University, Townsville,  
9 Queensland 4811, Australia

10 <sup>3</sup>NERC Isotope Geosciences Laboratory, British Geological Survey, Nottingham NG12 5GG,  
11 UK

12 <sup>4</sup>Department of Geology, University of Leicester, Leicester LE1 7RH, UK

13 <sup>5</sup>Anglo American Exploration, P. O. Box 61587, Marshalltown 2107, South Africa

14 <sup>6</sup>School of Earth and Environmental Sciences, The University of Queensland, Brisbane,  
15 Queensland 4072, Australia

16 <sup>7</sup>Isotope Geoscience Unit, Scottish Universities Environmental Research Centre (SUERC),  
17 Rankine Avenue, East Kilbride, Scotland, G75 0QF, UK

18 <sup>8</sup>Department of Earth & Environmental Science, School of Geography & Geosciences,  
19 University of St Andrews, St Andrews, KY16 9AJ, UK

20  
21 corresponding author: rholm@frogtech.com.au

22  
23 Keywords: Papua New Guinea; Solomon Islands; copper; gold; metallogensis; tectonic  
24 reconstruction

25

**Abstract**26  
27  
28  
29  
30  
31  
32  
33  
34  
35  
36  
37  
38  
39  
40  
41  
42  
43  
44  
45  
46  
47  
48  
49  
50

Papua New Guinea and the Solomon Islands are in one of the most prospective regions for intrusion-related mineral deposits. However, because of the tectonic complexity of the region and the lack of comprehensive regional geological datasets, the link between mineralization and the regional-scale geodynamic framework has not been understood. Here we present a new model for the metallogenesis of the region based on a synthesis of recent studies on the petrogenesis of magmatic arcs and the history of subduction zones throughout the region, combined with the spatio-temporal distribution of intrusion-related mineral deposits, and six new deposit ages. Convergence at the Pacific-Australia plate boundary was accommodated, from at least 45 Ma, by subduction at the Melanesian trench, with related Melanesian arc magmatism. The arrival of the Ontong Java Plateau at the trench at ca. 26 Ma resulted in cessation of subduction, immediately followed by formation of Cu-Au porphyry-epithermal deposits (at 24-20 Ma) throughout the Melanesian arc. Late Oligocene to early Miocene tectonic reorganization led to initiation of subduction at the Pocklington trough, and onset of magmatism in the Maramuni arc. The arrival of the Australian continent at the Pocklington trough by 12 Ma resulted in continental collision and ore deposit formation (from 12 to 6 Ma). This is represented by Cu-Au porphyry deposits in the New Guinea Orogen, and epithermal Au systems in the Papuan Peninsula. From 6 Ma, crustal delamination in Papua New Guinea, related to the prior Pocklington trough subduction resulted in adiabatic mantle melting with emplacement of diverse Cu and Au porphyry and epithermal deposits within the Papuan Fold and Thrust Belt and Papuan Peninsula from 6 Ma to the present day. Subduction at the New Britain and San Cristobal trenches from ca. 10 Ma resulted in an escalation in tectonic complexity and the onset of microplate tectonics in eastern Papua New Guinea and the Solomon Islands. This is reflected in the formation of diverse and discrete geodynamic

51 settings for mineralization within the recent to modern arc setting, primarily related to upper  
52 plate shortening and extension and the spatial relationship to structures within the subducting  
53 slab.

54

## 55 **1. Introduction**

56

57 The region of Papua New Guinea and Solomon Islands hosts an abundance of porphyry,  
58 epithermal and skarn mineral deposits, such as Ok Tedi, Frieda River, Porgera, Wafi-Golpu,  
59 Ladolam (Lihir) and Panguna (Bougainville; Fig. 1; Cooke et al., 2005; Sillitoe, 2010;  
60 Richards, 2013). Globally, such mineral-systems account for approximately one-fifth of the  
61 world's gold (Au) and nearly three-quarters of the world's copper (Cu) resources (Cooke et  
62 al., 2005; Sillitoe, 2010). Formation of these types of deposits is considered to be genetically  
63 linked to intermediate to felsic intrusive arc magmatism, typified by regions such as the  
64 North American Cordillera, the Andean margin of South America and the Tethyan Belt of  
65 Eurasia (e.g. Cooke et al., 2005; Sillitoe, 2010; Richards, 2013; Richards and Holm, 2013;  
66 Butterworth et al., 2016). The general relationship between porphyry-epithermal  
67 mineralization and subduction zones across the globe implies that there are broad, plate  
68 margin-scale tectono-magmatic controls on where and when these deposits form in the crust  
69 (e.g. Richards, 2003; Cooke et al., 2005). In particular, changes in the subduction regime are  
70 commonly considered as crucial parameters triggering mineralizing events, for example,  
71 associated with terrane collisions, subduction of slab structure (e.g., aseismic ridge), or  
72 changes in the slab angle during subduction (Cooke et al., 2005; Rosenbaum et al., 2005;  
73 Sillitoe, 2010; Rosenbaum and Mo, 2011; Richards, 2013; Richards and Holm, 2013). A  
74 detailed understanding of the geological settings linked to deposit emplacement is required  
75 when mineral exploration progresses to target concealed deposits beneath cover. This needs

76 to be applied at all scales, but we draw particular attention to the need for an appreciation of  
77 regional tectonics and the inherent tectonic complexities that arise through time that may be  
78 favorable for deposit emplacement.

79

80 The present-day geodynamic setting of Papua New Guinea and the Solomon Islands is a  
81 complex zone of oblique convergence at the boundary between the Australian and Pacific  
82 plates, trapped between the converging Ontong Java Plateau and Australian continent (Fig.  
83 2). The general tectonic framework of the southwest Pacific has been discussed in previous  
84 studies (e.g. Hall, 2002; Schellart et al., 2006), but there are still major uncertainties  
85 regarding the complex geodynamics of Papua New Guinea and Solomon Islands (e.g. Hall,  
86 2002; Holm et al., 2016). In addition, current geological and ore deposit datasets for this area  
87 are inadequate to inform meaningful conclusions. This study takes a high-level approach to  
88 this problem by addressing metallogenesis in terms of regional metal endowment and  
89 mineralization-styles rather than emphasizing the details of individual deposits or ore system-  
90 scale mechanisms for generation of mineral concentrations.

91

92 Recent work investigating the petrogenesis of magmatic arcs throughout the Papua New  
93 Guinea and Solomon Islands region (Schuth et al., 2009; Woodhead et al., 2010; Holm and  
94 Richards, 2013; Holm et al., 2013, 2015b), combined with regional plate tectonic modelling  
95 (Holm et al., 2016), provide a framework for us to develop a regional metallogenic model. In  
96 this study we build on the preliminary work of Holm et al. (2015a) to test the hypothesis that  
97 subduction-related ore deposits have formed under special circumstances, for example,  
98 related to terrane collision, ridge subduction or slab tearing. To achieve this, we combine  
99 information on subduction processes and arc magmatism with the distribution of mineral  
100 deposits, the styles of mineralization, and the timing of mineralization. We also present new

101 age dates on deposits and prospects. This allows us to provide a more comprehensive  
102 regional model for the formation of intrusion-related porphyry and epithermal deposits in the  
103 Papua New Guinea and Solomon Islands region through time, with implications for future  
104 exploration strategies.

105

## 106 **2. Tectonic Setting**

107

108 The Papua New Guinea mainland is composed of multiple terranes that were accreted to the  
109 northern Australian continental margin during the Cenozoic (e.g. Hill & Hall 2003;  
110 Crowhurst et al., 2004; Davies, 2012; Holm et al., 2015b). The result is an accretionary  
111 orogen characterized by sedimentary cover rocks on Australian continental crust (Papuan  
112 Fold and Thrust Belt; Dow, 1977; Hill and Gleadow, 1989; Craig and Warvakai, 2009),  
113 which is buttressed against variably deformed sedimentary, metamorphic and crystalline  
114 rocks of the composite New Guinea Mobile Belt (Fig. 2; Dow et al., 1972; Dow, 1977;  
115 Hutchison and Norvick, 1980; Hill and Raza, 1999; Davies, 2012). Together the Papuan Fold  
116 and Thrust Belt and the New Guinea Mobile Belt comprise the New Guinea Orogen. In  
117 contrast, the islands of eastern Papua New Guinea and the Solomon Islands represent island  
118 arc terranes formed adjacent to the Australia-Pacific plate boundary (Abbott, 1995; Hall,  
119 2002; Lindley, 2006; Holm et al., 2016). More detailed reviews of the regional tectonics can  
120 be found in Baldwin et al. (2012) and Holm et al. (2016), and references therein.

121

122 To the east of Papua New Guinea, plate convergence is currently accommodated by  
123 subduction of the Australian and Solomon Sea plates at the San Cristobal and New Britain  
124 trenches, respectively (Fig. 2). Magmatism associated with these subduction zones occurs in  
125 the Solomon arc, the Tanga-Lihir-Tabar-Feni chain and the New Britain arc, overprinting

126 Melanesian arc basement related to earlier subduction at the Melanesian trench (Woodhead et  
127 al., 1998; Petterson et al., 1999; Holm et al., 2013). The western extension of the New Britain  
128 trench and New Britain arc are the north-dipping Ramu-Markham fault zone, and the West  
129 Bismarck arc, respectively (Fig. 2; Abbott, 1995; Woodhead et al., 2010; Holm and Richards,  
130 2013).

131  
132 Active rifting and seafloor spreading occur in the Bismarck Sea back-arc basin, which  
133 comprises the North Bismarck and South Bismarck microplates, separated by the left-lateral  
134 strike-slip Bismarck Sea fault (Fig. 2; Denham 1969; Taylor 1979; Cooper and Taylor, 1987;  
135 Holm et al., 2016). The Woodlark Basin is an active extensional basin (Fig. 2) that began  
136 rifting at ca. 6 Ma (Taylor et al., 1995, 1999; Holm et al., 2016). To the west of the Woodlark  
137 Basin oceanic spreading gradually transitions to continental rifting of the Papuan Peninsula  
138 (Benes et al., 1994; Taylor, et al., 1995, 1999). Young oceanic crust, including the active  
139 Woodlark spreading center, are currently subducting to the northeast at the San Cristobal  
140 trench (Mann et al., 1998; Chadwick et al., 2009; Schuth et al., 2009).

141  
142 The Papua New Guinea and Solomon Islands region also preserves several subduction zones  
143 that are either extinct or accommodate only minor convergence at the present day. The  
144 Melanesian trench accommodated southwest-dipping subduction of the Pacific plate beneath  
145 the Australian plate and is associated with magmatism of the Melanesian arc (Petterson et al.,  
146 1999; Hall, 2002; Schellart et al., 2006; Holm et al., 2013). The location and orientation of  
147 subduction beneath the Papua New Guinea mainland that gave rise to the early to late  
148 Miocene Maramuni arc (Dow, 1977; Weiland, 1999), is by comparison a more contentious  
149 element of the regional tectonics (see Hall and Spakman, 2002; Holm et al., 2015b; Holm et  
150 al., 2016, and references therein). Here, we adopt the model that suggests that subduction at

151 the Pocklington trough (and the westward extension thereof into Papua New Guinea) gave  
152 rise to tectono-magmatic phenomena within Papua New Guinea and the Maramuni arc (e.g.  
153 Dow, 1977; Webb et al., 2014; Holm et al., 2015b). An alternative model invoking  
154 subduction at the Trobriand trough will be discussed below. At present, the Pocklington  
155 trough marks the southern margin of the Woodlark Basin. The interpreted western extension  
156 of this structure includes the Aure-Moresby trough southwest of the Papuan Peninsula (e.g.  
157 Ott and Mann, 2015), which forms a suture between the Papuan Fold and Thrust Belt and the  
158 New Guinea Mobile Belt (Fig. 2; e.g. Dow et al., 1972; Dow, 1977; Holm et al., 2015b). This  
159 proto-Pocklington trough is considered to represent a relict trench that accommodated north-  
160 dipping subduction of the Australian plate beneath New Guinea (Hill and Hall 2003; Cloos et  
161 al., 2005; Webb et al., 2014; Holm et al., 2015b), but may accommodate some recent  
162 convergence (e.g. Ott and Mann, 2015). The Trobriand trough marks the southern margin of  
163 the Solomon Sea (Fig. 2), which according to plate reconstructions (Holm et al., 2016), was  
164 an active subduction zone during the Pliocene (but not in the Miocene). No arc magmatism  
165 has been attributed to subduction at the Trobriand trough.

166

### 167 **3. Mineral Deposits**

168

169 Research on mineral deposits in the Papua New Guinea and Solomon Islands region has been  
170 mainly focused on the nature and controls of individual deposits and their district-scale  
171 setting (e.g. Richards and Ledlie, 1993; Hill et al., 2002; Gow and Walshe, 2005; Tapster et  
172 al., 2016). To investigate relationships between the evolution of the subduction arcs and the  
173 metallogensis of intrusion-related mineral deposits, we used data available from 47  
174 Cenozoic intrusion-related Cu-Au deposits (Table 1; Figs. 1 and 3), encompassing active  
175 mines, deposits and prospects. Our dataset has information on deposit style and the total



176 deposit endowment, including deposit tonnage, and copper and gold grades (Fig. 3). Metal  
177 endowment for each deposit was calculated based on deposit tonnage and metal grade. Data  
178 were sourced from recent company reports where possible, and were supplemented by data  
179 from Garwin et al. (2005), Singer et al. (2008) and other relevant literature (see Table 1;  
180 reported deposit information is not intended as a JORC-compliant category; deposit  
181 endowment references are included in the supplementary material).

182  
183 The geochronological dataset is supplemented by new radiometric constraints for six  
184 deposits. Additional constraints are based on field observations and stratigraphic  
185 relationships. Uncertainties within the dataset originate from both parametric sources (quoted  
186 uncertainty due to analysis and systematic uncertainties e.g. decay constants), and non-  
187 parametric geological uncertainty, for example, the difference between the dated igneous  
188 intrusion and the hydrothermal system or alteration episode.

189  
190 Mineral deposits throughout the Papua New Guinea and Solomon Islands region range in age  
191 from late Oligocene to Quaternary (Table 1; Fig 1). The age of copper and gold mineral  
192 deposits in mainland Papua New Guinea ranges from Miocene to Quaternary. These deposits  
193 are dominated by porphyry-type deposits, which formed within the New Guinea Orogen (e.g.,  
194 Ok Tedi, Frieda River, Porgera, Wafi-Golpu; Fig. 1). Epithermal- and porphyry-type  
195 deposits, such as Hidden Valley (Papua New Guinea) and Tolukuma, occur along the Papuan  
196 Peninsula and extend east into the Woodlark Basin (Umuna, Misima Island and Woodlark  
197 deposits). Commodities throughout mainland Papua New Guinea vary between copper-rich  
198 and gold-rich deposits (Figs. 1 and 3). The islands in eastern Papua New Guinea and the  
199 Solomon Islands represent island arc settings with deposits ranging from Oligocene to recent  
200 ages. These deposits occur as porphyry- and epithermal-type deposits, as well as seafloor

201 massive sulphide (SMS) deposits, with no clear trend in either copper or gold dominated  
202 systems (Figs. 1 and 3). Well-known deposits within this region are represented by the high-  
203 grade SMS Solwara deposits, and the giant Ladolam (Lihir) and Panguna (Bougainville)  
204 deposits.

205

#### 206 **4. Samples and Methodology**

207

##### 208 **4.1 Samples**

209

210 Six rock samples were obtained from mines, deposits and prospects for the purpose of  
211 gaining new geochronological constraints on the timing of deposit formation. The chosen  
212 samples represent either recently discovered mineralized localities with no timing constraint  
213 or historically identified mineral occurrences that have lacked conclusive age dating.

214

215 Two samples (109472a and JD15) are from Papua New Guinea (see Fig. 1). Sample 109472a,  
216 from the Ipi River porphyry Cu-Au-Mo and epithermal Au prospect (146.71°E 8.25°S), is an  
217 intensely stockworked, altered and mineralized porphyritic andesite. The prospect is located  
218 in the Owen Stanley Ranges of the central Papuan Peninsula, approximately 50 km northwest  
219 of the Tolukuma mine. Sample JD15 (668956 9341950 UTM AGD66 zone 54S) is from the  
220 Baia porphyry Cu-Au prospect located southwest of Porgera within the Papuan Fold and  
221 Thrust Belt. The sample is a crystal-rich lapilli tuff of andesitic composition, with complexly  
222 zoned plagioclase and minor hornblende in a fine-grained fragmental matrix. Both samples  
223 are derived from magmatic occurrences associated with mineralization and represent the  
224 probable maximum age for mineralization.

225

226 Sample SI11886 (6°51'49.24"S 156° 5'9.73"E; Turner and Ridgeway, 1982), from Fauro  
227 Island in the Solomon Islands, is a porphyritic hornblende-biotite dacite from the calc-  
228 alkaline volcanic sequence that was emplaced into a late Oligocene-early Miocene tholeiitic  
229 lava sequence associated with earlier Melanesian arc growth (Turner and Ridgeway, 1982). A  
230 number of high-grade epithermal Au-Ag prospects are hosted by the dacitic volcanism and  
231 likely share a genetic association. The dacitic volcanism has not previously been dated by  
232 radio-isotopic methods and no biostratigraphic ages are available, but some authors have  
233 proposed a potentially pre-Pliocene age (Turner and Ridgeway 1986).

234

235 The Choe Intrusive complex of southeast New Georgia is host to the Tirua Hill prospect (also  
236 known as Hube River). The complex represents a nested sequence of picritic gabbro-  
237 microgranite intrusives (Dunkley, 1986) that was emplaced into an island arc picritic basalt  
238 volcanic sequence. This sequence represents the earliest stages of island growth linked to  
239 initial Woodlark spreading ridge subduction (Rohrbach et al., 2005) so the intrusion age  
240 represents a minimum constraint on the timing of this tectonic event. The Tirua Hill Prospect  
241 contains minor occurrences of secondary biotite in association with pervasive sericitic and  
242 silicic alteration, zones of argillic alteration and a large propylitic halo, in addition to (Au,  
243 Ag, Cu, Pb, Zn) sulfide and sulfosalt minerals (Dunkley, 1986). Sample SI1059 (8°28'6.42"S  
244 157°47'53.63"E) is a diorite from this zone that postdates the picritic magmatism and  
245 contains a stockwork of oxidized pyritic stringers, representing a maximum age for  
246 mineralization.

247

248 The Sutakiki prospect is located in central Guadalcanal and lies ~10 km north-northeast of  
249 the ca. 1.6-1.45 Ma plutonic Koloula Porphyry prospect (Tapster et al., 2016) and ~10 km  
250 south-southwest from the low-sulphidation epithermal Gold Ridge Mine, along the strike of

251 an arc-normal structural corridor (Hackman 1980; Swiridiuk, 1998, Tapster et al., 2011). The  
252 prospect is hosted by sheared ophiolitic mafic rocks and limestones and contains a range of  
253 high-grade Au epithermal and skarn mineralization and porphyry-style alteration, hosted by a  
254 porphyritic intrusion intersected within drill core. Sample SK001\_346-346.27m  
255 ( $9^{\circ}41'26.37''\text{S}$   $160^{\circ}4'58.50''\text{E}$ ) is a porphyritic hornblende diorite that has weak propylitic  
256 alteration and contains minor stringers of pyrite and chalcopyrite, with the age of intrusion  
257 taken to represent the maximum age for mineralization but with a close genetic association  
258 between magmatic and hydrothermal systems in the area.

259  
260 Gold Ridge Mine, Guadalcanal is hosted by a supra-crustal volcanoclastic infill of a fault  
261 controlled rhombohedral basin that lies at the north-northeast extent of the arc-normal  
262 structural corridor that also contains the Sutakiki and Koloula Prospects (Hackman, 1980;  
263 Swiridiuk, 1998). The ore body contains Au, primarily hosted as native Au and electrum,  
264 found in association with chalcopyrite, galena, sphalerite, pyrite-marcasite, and arsenopyrite.  
265 Two samples, GDC3 279.45 and GDC5 45.8 ( $9^{\circ}35'25.90''\text{S}$ ,  $160^{\circ}7'44.01''\text{E}$ ), with quartz-  
266 adularia-carbonate-sulfide assemblages, probably reflecting the “stage-1” 266-280°C veins  
267 (Corbett and Leach, 1998) were selected for Ar-Ar dating of adularia from the upper and  
268 lower sections of the orebody that was intersected in recent (2013) drill holes in the  
269 Charivunga Gorge Extension.

270

#### 271 **4.2 U-Pb geochronology**

272

273 U-Pb dating was conducted on magmatic zircon grains associated with intrusion-related  
274 deposits and prospects. Zircon grains were separated from hand samples or drill cores using  
275 standard techniques. They were then handpicked under a binocular microscope and imaged

276 using cathodoluminescence (CL). Zircon U-Pb geochronology analyses for samples from  
277 Papua New Guinea were conducted at the Advanced Analytical Centre of James Cook  
278 University using a Coherent GeolasPro 193 nm ArF Excimer laser ablation system connected  
279 to a Bruker 820-ICP-MS (for methodology, see Holm et al. 2013, 2015b). Zircon grains from  
280 the Solomon Islands, with the exception of SI11886, were analyzed for U-Pb geochronology  
281 using a Nu Instruments Attom HR single-collector inductively coupled plasma mass  
282 spectrometer (HR-ICP-MS) with laser ablation performed by a New Wave Research UP193ss  
283 laser (NERC Isotope Geosciences Laboratories, British Geological Survey; see Tapster et al.  
284 2014 for methodology). Sample SI11886 was analyzed using a Nu Plasma HR multi-collector  
285 ICP-MS, following the methods of Thomas et al. (2016). Further information on data  
286 collection, validation and reduction are provided in the supplementary materials.

287

### 288 **4.3 Ar-Ar geochronology**

289

290 Following sample screening and petrographic studies, Gold Ridge adularia was identified  
291 within <2 cm composite veinlets, as <500  $\mu\text{m}$ -sized crystals that are inter-grown with quartz  
292 and carbonate minerals. The fine-grained nature of the target minerals and cm-scale vein size  
293 that was intercalated with wall rock material required development of a non-standard  
294 procedure to extract clean adularia separates for irradiation and Ar-Ar analyses. Samples  
295 were initially cut to remove as much of the host material adhered to the vein as possible, this  
296 was then leached in a warm bath of weak citric acid to reduce the calcite within the vein and  
297 aide disaggregation. The acid was frequently replaced until no effervescence occurred when  
298 the fresh acid was introduced. Following hand-crushing, sieving, washing, and  
299 electromagnetic separation, non-magnetic fractions 355-500  $\mu\text{m}$  were passed through LST  
300 (lithium polytungstates) heavy liquids twice at the required densities to initially remove pyrite

301 and then to remove quartz. The appropriate density fraction was then laid in a grid formation  
302 on carbon tape and examined under environmental mode SEM to screen the remaining  
303 grains; this was an important step as grains were commonly composite quartz-adularia, or had  
304 clear Na peaks, suggesting that the feldspar was likely to be derived from the feldspathic-  
305 altered wall rock material rather than primary hydrothermal adularia. The best grains were  
306 selected and removed from the carbon tape to form the mineral separate. Mineral separates  
307 were irradiated at the Cd-lined McMaster facility, Ontario, Canada, for 5 minutes after being  
308 packaged into Al-discs. J values were calculated via the irradiation of Alder Creek Sanadine  
309 ( $1.1891 \pm 0.0006$  Ma; Niespolo et al., 2016). Samples were analysed at Scottish Universities  
310 Environmental Research Council facility, East Kilbride. Full details on the analytical  
311 procedures are described in the supplementary information.

312

### 313 **5. Geochronology Results**

314

315 Results for zircon U–Pb age dating for the selected samples from Ipi River, Baia, Fauro  
316 Island, Tirua and Sutakiki are shown in Figure 4, and Ar–Ar adularia ages for Gold Ridge are  
317 shown in Figure 5. These final interpreted ages are also included in Table 1. The results do  
318 not show evidence for significant isotopic disturbance or mixing of different age domains  
319 during zircon ablation, nor is there any significant difference in the age of zircon cores and  
320 rims. The complete zircon isotopic data can be found in the supplementary material.

321

322 All interpreted magmatic crystallization ages are Pliocene to Quaternary. Uncertainties are  
323 reported at a  $2\sigma$  level with a minimum uncertainty reported at 0.1 Myr. Sample 109472a from  
324 Ipi River yielded a crystallization age of  $4.9 \pm 0.1$  Ma (N=14; MSWD=1.4); sample JD15  
325 from Baia returned an age of  $1.70 \pm 0.1$  Ma (N=24; MSWD=1.4). The Tirua Hill sample

326 SI1059 yielded an age of  $2.4 \pm 0.1$  Ma (N=20; MSWD=1.1); the Fauro Island sample,  
327 SI11886, returned an age of  $3.4 \pm 0.2$  Ma (N=8; MSWD=2.2); sample SK001\_346-346.27m  
328 from Sutakiki yielded an age of  $1.54 \pm 0.1$  Ma (N=10; MSWD=1.4).

329

330 The two Adularia bearing vein samples from the Gold Ridge Mine yielded 100% plateau ages  
331 of  $1.63 \pm 0.05/0.06$  Ma and  $1.51 \pm 0.09/0.09$  Ma, (quoted at  $1\sigma$  with the latter value including  
332 decay constant uncertainties) and are indistinguishable within uncertainty. Data precision is  
333 controlled by the large degree of atmospheric contamination.

334

## 335 **6. Plate Tectonic Reconstructions**

336

337 Plate tectonic reconstructions allow us to observe and test relationships between major  
338 tectonic events and the location and timing of mineral deposit formation. The reconstructions  
339 of this study build on the work by Holm et al. (2015a, 2016) but are extended back to 30 Ma  
340 to encompass the main regional ore-forming events. The plate tectonic reconstructions (Figs.  
341 6, 7 and 8) were developed using GPlates software (e.g. Boyden et al., 2011; Seton et al.,  
342 2012). Plate kinematics were resolved relative to the global moving hotspot reference frame  
343 (Müller et al., 2016) using the regional plate motion framework from prior reconstructions  
344 (Seton et al., 2012; Holm et al., 2016; Müller et al., 2016). The reconstructions (Figs. 6, 7 and  
345 8) are presented in relative reference frames for ease of visualization. These reconstructions  
346 were simplified and are mainly aimed at emphasizing major tectonic reorganization events  
347 associated with the evolution of the Melanesian arc, Maramuni arc, and New Britain and  
348 Solomon arcs. The plate features and rotation files for these reconstructions are available in  
349 the supplementary material. The development of detailed plate tectonic reconstructions for  
350 the region is beyond the scope of this study.

351

352 A range of datasets and models specific to the Papua New Guinea and Solomon Islands  
353 region were incorporated in the reconstructions (see Holm et al., 2016 for details). To extend  
354 the plate reconstructions back to 30 Ma, the previous dataset was expanded using constraints  
355 on the timing of major plate boundary events (e.g. Cloos et al., 2005; Knesel et al., 2008;  
356 Holm et al., 2015b). In this study we make the assumption that subduction of the Pacific plate  
357 was occurring at the Melanesian trench from ca. 45 Ma and all upper plates were fixed to the  
358 Australian plate motion. Collision of the Ontong Java Plateau with the Solomon Islands at ca.  
359 26 Ma (Pettersen et al., 1999; Knesel et al., 2008; Holm et al., 2013) terminated convergence  
360 between the Pacific plate and Solomon arc. This collision event, combined with  
361 contemporaneous arc-continent collision between the New Guinea Mobile Belt and Sepik  
362 Arc in the late Oligocene (not shown; Dow, 1977; Crowhurst et al., 1996), is interpreted to  
363 result in a shift of regional convergence to subduction at the Pocklington trough. At this time,  
364 the composite New Guinea Mobile Belt terrane and Solomon Sea became fixed to the Pacific  
365 plate motion. At ca. 12 Ma, collision of the Australian continent with the New Guinea Mobile  
366 Belt closed the Pocklington Sea, but subduction did not initiate at the New Britain-San  
367 Cristobal trench until ca. 10 Ma. Because of the limitations of rigid plate behavior we assume  
368 that 10 Ma was the timing of complete cessation of convergence at the Pocklington trough  
369 and initiation of subduction at the New Britain-San Cristobal trench. After 10 Ma, the New  
370 Guinea Mobile Belt and Solomon Sea plate motion were fixed to the Australian plate, until  
371 the onset of regional microplate tectonics from ca. 6 Ma (Holm et al. 2016).

372

373 The plate tectonic reconstructions were then correlated with the formation of mineral deposits  
374 in time and space. The timing and location of deposit formation is according to Table 1,  
375 where these are assigned to 3-million-year time windows. In the following section, we outline



376 the tectonic evolution of the magmatic arcs of the Papua New Guinea and Solomon Islands  
377 region, and correlate episodes of mineral deposit formation with major tectonic events,  
378 utilizing the plate tectonic reconstructions. The role of structures, both in the upper plate and  
379 as slab structures is also introduced, however, this can only be correlated for the active and  
380 recent metallogenic systems where we have sufficient insight into the morphology and  
381 structure of the subducting plate. Such relationships between tectonics and deposit formation  
382 provided by this review of regional metallogenesis can provide a guide to the recognition of  
383 similar patterns in ancient convergent margins and serve to inform future exploration  
384 strategies.

385

## 386 **7. Regional Metallogenesis**

387

### 388 **7.1 Tectonic evolution and metallogenesis of the Melanesian arc**

389

390 The Melanesian arc, comprised of New Britain, New Ireland and Bougainville of Papua New  
391 Guinea, and much of the Solomon Islands (e.g. Abbott, 1995; Kroenke, 1984; Petterson et al.,  
392 1999), represents the expression of arc magmatism related to subduction of the Pacific plate  
393 beneath the Australian plate at the Melanesian trench (Figs. 2 and 6; Petterson et al., 1999;  
394 Hall, 2002; Schellart et al., 2006; Holm et al., 2013). The early stages of subduction and arc  
395 development are poorly understood due to the paucity of known exposed Melanesian arc  
396 rocks and limited studies to date. Since the time of arc formation, however, Melanesian arc  
397 basement has undergone complex tectonic reorganizations (Petterson et al., 1999; Hall, 2002;  
398 Schellart et al., 2006; Holm et al., 2016).

399

400 The most significant event in the history of the Melanesian arc is the collision of the 33 km  
401 thick Cretaceous Ontong Java Plateau with the Australian plate margin in the vicinity of the  
402 Solomon Islands (Kroenke, 1984; Petterson et al., 1999) at approximately 26 Ma (Fig. 6;  
403 Petterson et al., 1999; Hall, 2002; Knesel et al., 2008; Holm et al., 2013). This collision is  
404 interpreted to have caused 1) deceleration of the Australian plate motion (Knesel et al., 2008);  
405 2) cessation of sea floor spreading in the Caroline Sea, Solomon Sea, Rennell trough and  
406 South Fiji Basin at or around 25 Ma (Davey, 1982; Hall, 2002; Gaina and Müller, 2007;  
407 Seton et al., 2016); 3) termination of magmatism in (at least) the western Melanesian arc in  
408 the earliest Miocene (Petterson et al., 1999; Lindley, 2006; Holm et al., 2013); and 4) opening  
409 of a series of intra-arc basins along the same arc from approximately the late Oligocene  
410 (Central Solomon Basin [Cowley et al., 2004; Wells, 1989]; New Hebrides intra-arc basins  
411 [Bradshaw, 1992]). Locally in New Britain, an early Miocene extensional regime is inferred  
412 from north-northeasterly extensional joint sets and associated hydrothermal activity dated at  
413 22–23 Ma (Wilcox et al., 1973; Lindley, 2006).

414

415 Following Ontong Java collision, intense metallogenic activity occurred in the Melanesian  
416 arc. Mineral deposits are spatially distributed throughout the Melanesian arc in regions where  
417 the arc rocks of this age are outcropping (Fig. 6). The mineral deposits are distributed both  
418 adjacent to the site of Ontong Java Plateau collision (Guadalcanal and New Ireland), and  
419 distal to collision (New Britain). This suggests that mineralization was likely an arc-scale  
420 event rather than a more local process associated directly with plateau collision and stagnant  
421 or flat slab subduction (e.g. Kay and Mpodozis, 2001; Rosenbaum et al., 2005). Most  
422 deposits are porphyry Cu deposits with subsidiary epithermal deposit types; Au features  
423 mainly as a secondary commodity (Fig. 6). It is unclear whether this is a function of  
424 exhumation (e.g. erosion of high-level epithermal deposits) and currently exposed crustal

425 levels, or whether this is influenced by the magma composition and localized fluid  
426 characteristics. The timing of formation of most Melanesian arc deposits is unfortunately  
427 poorly constrained, but based on the known interpreted deposit ages it appears that the main  
428 metallogenic episode formed shortly after the collision of the Ontong Java Plateau with the  
429 Solomon Islands(ca 24-20 Ma).

430

431 Few studies have investigated the late Oligocene-early Miocene Cu-Au mineralization within  
432 the Melanesian arc making it difficult to correlate deposit formation with specific  
433 mechanisms within the arc setting. However, post-collision mineralizing intrusions related to  
434 formation of the Simuku deposit in New Britain have been shown to hold adakite-like  
435 characteristics (e.g. high Sr/Y, HREE depletion; Holm et al. 2013). Such affinities are  
436 commonly linked to intrusion-related mineral deposits globally (e.g. Richards, 2011; Loucks,  
437 2014). The mechanism for generating these intrusions is not yet conclusive, but Holm et al.  
438 (2013) interpreted that the intrusions must have originated from mantle-derived melt at high  
439 pressure (i.e. deep crust or mantle) or melting of a garnet-bearing source, such as eclogite or  
440 garnet amphibolite of the subducting slab or thickened arc crust (Chiaradia, 2009; Chiaradia  
441 et al., 2009; Macpherson et al., 2006; Rapp and Watson, 1995; Richards, 2011; Richards and  
442 Kerrich, 2007; Sen and Dunn, 1994).

443

## 444 **7.2 Tectonic evolution and metallogenesis of the Maramuni arc**

445

446 Following the arrival of the Ontong Java Plateau at the Melanesian trench, at 26 Ma  
447 (Pettersen et al., 1999; Knesel et al., 2008; Holm et al., 2013), and late Oligocene arc-  
448 continent collision of the Sepik arc terranes onto the northern margin of the New Guinea  
449 Mobile Belt (Dow, 1977; Pigram and Davies, 1987; Struckmeyer et al., 1993; Abbott et al.,

1994; Abbott, 1995; Crowhurst et al., 1996; Findlay, 2003), Maramuni arc magmatism  
intruded the New Guinea Mobile belt from the early Miocene (Dow et al., 1972; Page, 1976;  
Dow, 1977). As outlined above, the subduction that gave rise to the Maramuni arc is  
contentious, and we adopt a model of north-dipping subduction at Pocklington trough to the  
south of the New Guinea Mobile Belt and Papuan Peninsula (Holm et al., 2015b; a similar  
inference was also made by Cloos et al. (2005) and Webb et al. (2014)). However, the extent  
of this structure west into Indonesia is unclear. At this time (late Oligocene-early Miocene),  
the New Guinea Mobile Belt existed as a ribbon of marginal continental crust (e.g. Crowhurst  
et al., 2004) that was rifted from the Australian continent, perhaps somewhat analogous to the  
modern-day Lord Howe Rise and Norfolk Ridge in the Tasman Sea. There are no known  
significant mineral deposits formed during this first phase of arc magmatism (Fig. 7).

By ca. 12 Ma, convergence at the Pocklington trough and northward drift of the Australian  
continent resulted in collision with the outboard New Guinea Mobile Belt and the closure of  
the Pocklington Sea (Fig. 7; Cloos et al., 2005; Webb et al., 2014; Holm et al., 2015b). This  
event is marked by uplift in the New Guinea Orogen (Hill and Raza, 1999; Cloos et al.,  
2005). This change is also manifested in the magmatic record by a transition from medium-K  
calc-alkaline arc magmatism at ca. 12 Ma to a marked increase in crustal contribution to the  
magmas and less positive  $\epsilon_{\text{Hf}}$  values at ca. 9.4 Ma and 8.7 Ma, interpreted as introduction of  
Australian crust into the subduction zone (Holm et al., 2015b). From 12 Ma, growth of the  
New Guinea Orogen was driven by shortening and uplift of the New Guinea Mobile Belt and  
by accretion of Australian continental platform sediments that initiated the accretionary  
complex of the Papuan Fold and Thrust Belt (Hill and Gleadow, 1989; Hill et al., 2002; Cloos  
et al., 2005; Holm et al., 2015b).

474

475 Syn-orogenic magmatism of the Maramuni arc was associated with the formation of  
476 extensive 12-6 Ma mineral systems throughout mainland Papua New Guinea (Fig. 7). These  
477 deposits form a belt proximal to the site of continental collision (Lagaip and Bundi fault  
478 zones; Figs. 2 and 7), which forms the suture between the Papuan Fold and Thrust Belt and  
479 the New Guinea Mobile Belt (Dow et al., 1972; Dow, 1977; Holm et al., 2015b). The  
480 Woodlark deposit, located on the offshore extension of the Papuan Peninsula, is temporally  
481 correlative with deposits on mainland Papua New Guinea and is therefore included in this  
482 group (Figs. 1 and 7). In general, the earlier deposits associated with this metallogenic  
483 episode, which formed at ca. 12 Ma (e.g., Frieda River, Wamum and Woodlark Island),  
484 reside in the New Guinea Mobile Belt to the north of the main collisional suture, whereas the  
485 later deposits (e.g. Yandera, Kainantu and Wafi-Golpu) reside adjacent to the Lagaip and  
486 Bundi suture zones (Fig. 1). This spatial-temporal distribution is in agreement with the  
487 interpreted tectonic model of southward migrating arc magmatism (Fig. 2; Davies, 1990) in  
488 response to continental underthrusting and slab steepening (Cloos et al., 2005; Holm et al.,  
489 2015b). Mainland deposit types are typically porphyry deposits, as opposed to epithermal  
490 deposits that occur farther east on the Papuan Peninsula (Fig. 7). This may reflect variation in  
491 the level of exhumation and erosion with deeper crustal levels exposed in the New Guinea  
492 Orogen related to greater crustal shortening and uplift. In addition, there is also an observed  
493 change in the nature of mineral resources, with Cu-Au mineral systems dominating the New  
494 Guinea Orogen, whereas Au systems are more dominant farther east on the Papuan Peninsula  
495 to Woodlark Island (Fig. 7). This also correlates with a spatial change in the nature of  
496 magmatic activity, with medium-K calc-alkaline magmatism of the New Guinea Orogen  
497 transitioning to high-K calc-alkaline magmatism in southeast Papua New Guinea (e.g. Smith,  
498 1976; Ashley and Flood, 1981; Whalen et al., 1982; Lunge, 2013; Holm et al., 2015b)  
499

500 From approximately 7 Ma, uplift of the New Guinea Orogen and the apparent intensity of  
501 magmatism accelerated (Hill and Gleadow, 1989; Cloos et al., 2005). Magmatism of this age  
502 shows a clear migration to the south, forming a latest Miocene–Quaternary magmatic belt  
503 that intruded the Papuan Fold-and-Thrust Belt and the Fly Platform to the south (Fig. 2).  
504 Recent and preserved Quaternary magmatism is expressed as widespread large shoshonitic  
505 and andesitic stratovolcanoes and intrusive bodies (Page, 1976, Johnson et al., 1978), often  
506 spatially controlled by regional-scale structural lineaments (Davies, 1990; Hill et al., 2002).  
507 This magmatism is often characterized by a HREE-depleted composition indicative of melt  
508 generation or fractionation at high-pressure in the presence of garnet (Holm et al., 2015b).  
509 While investigations into the source of this magmatism has been inconclusive to date (e.g.  
510 Johnson et al., 1978; Johnson and Jaques, 1980), the most likely scenario is that post-  
511 orogenic melting was triggered by adiabatic decompression of the underlying asthenosphere  
512 in response to detachment of the stagnated Pocklington slab and collisional delamination at  
513 ca. 6 Ma (Cloos et al., 2005; Holm et al., 2015b). The current location of the detached  
514 Pocklington slab has not yet been investigated but the recognition of a high-velocity P-wave  
515 tomography anomaly beneath northern Australia (e.g. Hall and Spakman, 2002; Schellart and  
516 Spakman, 2015) may represent the detached slab.

517

518 Mineral deposits associated with the post-orogenic metallogenic episode are defined by ages  
519 of ca. 6 Ma and younger, and include deposits such as Porgera, Ok Tedi and Tolukuma (Fig.  
520 7). The spatial distribution of these deposits forms a general belt that reflects the geological  
521 setting of the earlier Maramuni arc magmatism but is more continuous along the New Guinea  
522 Orogen and Papuan Peninsula when compared to the earlier syn-orogenic deposits (Fig. 7).  
523 This behavior may be related to preservation. These post-orogenic deposits generally reside  
524 to the south of the 12-6 Ma deposits and are hosted within the Papuan Fold and Thrust Belt

525 and Papuan Peninsula but there is no clear spatial trend related to the age of deposit formation  
526 internally within this group. Intrusions related to mineralization are diverse in nature, for  
527 example, intraplate alkalic basalts that host the giant Porgera gold deposit (Richards et al.,  
528 1990) are distinct within the extensive shoshonitic and high-K calc-alkaline post-orogenic  
529 magmatism (e.g. Smith, 1976, 1982; Johnson et al., 1978; van Dongen et al., 2010a; Holm  
530 and Poke, 2018). These differences highlight unexplained discrete geochemical domains  
531 within what appears to be a continuous magmatic belt. Deposits of this age are diverse and  
532 represented by porphyry and epithermal deposits with some related mineralized skarn  
533 systems. There is no clear preferred commodity type observed for the post-orogenic deposits.  
534 Gold deposits are widespread, particularly to the east (in the Papuan Peninsula). However, Cu  
535 appears to become more important in the central New Guinea Orogen with deposits such as  
536 Ok Tedi, Star Mountains and Baia (Fig. 7).

537  
538 In comparison to the subduction model presented here, the alternative model invokes  
539 southwest-dipping subduction at the Trobriand trough to the north of New Guinea from the  
540 late Oligocene (Crowhurst et al., 1996; Hill and Raza, 1999; Hall, 2002). The interpretation of  
541 the Trobriand trough and associated plate margin geometry has taken various forms (Fig. 7;  
542 e.g. Davies et al., 1987; Lock et al., 1987; Hall, 2002; Schellart et al., 2006; Davies, 2012;  
543 Seton et al., 2016). Arc-continent collision at the Trobriand trough plate boundary, often in  
544 combination with the sinistral transpression across northern New Guinea (Fig. 7), is then  
545 linked to the ongoing formation of the New Guinea Orogen and associated mineral deposit  
546 formation. However, given the late Oligocene age of initial docking of the Sepik arc terranes  
547 at the northern New Guinea coast, there is a large disconnect in time (and indeed in space)  
548 between the interpreted collision event and the onset of orogenesis and mineral deposit  
549 formation from 12 Ma. Together with the recent findings from Cloos et al. (2005), Webb et

550 al. (2014), and Holm et al. (2015b), this supports the use of the Pocklington trough  
551 subduction model over that of the Trobriand trough.

552

### 553 **7.3 Tectonic evolution and metallogenesis of the New Britain and Solomon arcs**

554

555 Following collision of the Australian continent with Papua New Guinea and cessation of  
556 subduction at the Pocklington trough (Cloos et al., 2005; Holm et al., 2015b) by ca. 10 Ma,  
557 the regional tectonics had undergone reorganization and convergence was established at the  
558 New Britain and San Cristobal trenches (e.g. Petterson et al., 1999). This period of tectonic  
559 reorganization is characterized by the ongoing development of regional microplate tectonics,  
560 marked by rapid changes in the plate kinematics of discrete terranes and the localized,  
561 simultaneous development of extensional and contractional tectonics.

562

563 Retreat of the western New Britain trench from ca. 6 Ma led to back-arc extension and rifting  
564 that initiated formation of the Bismarck Sea (Taylor, 1979; Holm et al., 2016). Anticlockwise  
565 rotation of the Solomon Sea, linked to hinge retreat at the western New Britain trench  
566 (Wallace et al., 2014; Ott and Mann, 2015; Holm et al., 2016), resulted in decoupling of the  
567 Solomon Sea plate from the Australian plate, which initiated minor underthrusting of the  
568 Solomon Sea plate at the Trobriand trough (Holm et al., 2016), and rotational extension and  
569 rifting in the Woodlark Basin from ca. 6 Ma (Taylor et al., 1999; Wallace et al., 2014; Holm  
570 et al., 2016). This period of tectonic reorganization from ca. 10 to 6 Ma reflects an overall  
571 setting dominated by extensional tectonics that does not seem to be linked to known mineral  
572 deposits.

573



574 Subduction of the active Woodlark spreading center at the San Cristobal trench from ca. 5 Ma  
575 had important implications for the geological evolution of the Solomon Islands (Chadwick et  
576 al., 2009; Holm et al., 2016). The timing for initial ridge subduction overlaps with the onset  
577 of crustal shortening across the Solomon Islands and convergence at the North Solomon  
578 trench adjacent to the Ontong Java Plateau (Petterson et al., 1997, 1999; Cowley et al., 2004;  
579 Mann and Taira, 2004; Phinney et al., 2004; Taira et al., 2004; Holm et al., 2016). Subduction  
580 of the spreading center adjacent to the central Solomon Islands also caused extensive arc  
581 magmatism, which included high-Mg andesites and adakite-like geochemical signatures  
582 (Mann et al., 1998; Chadwick et al., 2009; Schuth et al., 2009). This was exemplified by  
583 formation of the New Georgia group of islands that coincide with the location of spreading  
584 ridge subduction (Fig. 8; Petterson et al., 1999; Chadwick et al., 2009; Schuth et al., 2009;  
585 Holm et al., 2016), and host the Tirua, Mase and Kele River deposits (Figs. 1 and 8a).  
586 Reconstructions show that the New Georgia islands and associated ore deposits have been  
587 located adjacent to the subducting spreading center since at least the middle Pliocene (Fig.  
588 8a). The first absolute geochronological constraints from this area (Tirua Hill; Fig. 4) indicate  
589 that mineralization occurred around 2.4 Ma. Cross-cutting relationships with island arc  
590 picrites, which signify the effects of spreading ridge subduction on the arc magmatism,  
591 indicate that mineralization must post-date initial spreading ridge subduction. The slab  
592 window generated by spreading ridge subduction is potentially the cause of one of few  
593 currently active volcanic centers in the Solomon arc and a potentially mineralizing  
594 hydrothermal system at Savo Island (Smith et al., 2009, 2010, 2011). This suggests a  
595 prolonged (~2.5 Myr) influence of direct ridge subduction on magmatism and the formation  
596 of mineral deposits.

597

598 In addition to spreading center subduction, a correlation also exists for the location and  
599 timing of deposit formation with subduction of the Woodlark Basin marginal structures.  
600 Mineralization on Guadalcanal, at the southeast margin of the Woodlark Basin, occurred at  
601 ca. 1.6 Ma, approximately contemporaneously with the emplacement of the Koloula  
602 Porphyry Complex (1.6-1.45 Ma; Tapster et al., 2016), Sutakiki epithermal-porphyry  
603 prospect (1.5 Ma) and Gold Ridge low sulfidation epithermal deposit (1.6-1.5 Ma; Fig. 8b)  
604 along an arc-normal (NNE-SSW) transpressive structural corridor in central Guadalcanal  
605 (Hackman, 1980; Swiridiuk, 1998; Tapster et al., 2011, 2016). Given the nature of described  
606 fault-intrusion relationships at Koloula, the arc-normal deformation that controlled  
607 mineralization along the corridor was only active shortly before 1.6 Ma and had terminated  
608 by ca. 1.5 Ma (Tapster et al., 2016). The close temporal association of porphyry to epithermal  
609 deposits (~100 kyrs) along a spatial corridor that extends over 30 km preclude a direct  
610 genetic link between deposits and highlight the critical role that short-lived upper plate  
611 structures can have on controlling mineralization. The central NNE-SSW corridor in  
612 Guadalcanal runs parallel to a similar set of lineaments in the west of the island, currently  
613 under a much thicker Pliocene-Pleistocene volcanic cover. The orientation of structures  
614 across the island and their coincidence with the subduction of the southeast margin of the  
615 Woodlark Basin (Fig. 8b) suggests that there may be a relationship between the upper-plate  
616 structure and subducting topographic high (Tapster et al., 2011). Subduction of the young,  
617 hot and buoyant Woodlark Basin crust potentially acted as an indenter, generating structural  
618 controls for magma emplacement and mineralization. A similar relationship exists for the  
619 location of subduction of the northwest margin of the Woodlark Basin and formation of the  
620 Panguna and Fauro Island deposits in the adjacent overriding plate at ca. 3.5-3.4 Ma (Fig. 8a).  
621

622 Farther west, the Tabar-Lihir-Tanga-Feni island arc chain of eastern Papua New Guinea hosts  
623 the Ladolam, Simberi and Kabang deposits. In this area, differential plate motion between the  
624 Solomon Islands and the North Bismarck microplate resulted in intra-arc extension between  
625 the islands of New Ireland and Bougainville (Holm et al., 2016). An extensional origin for the  
626 Tabar-Lihir-Tanga-Feni island arc chain is supported by geochemical studies, which  
627 suggested that the volatile-rich, silica-undersaturated, high-K calc-alkaline basaltic lavas  
628 were produced by adiabatic decompression melting of subduction-modified upper mantle  
629 (Patterson et al., 1997; Stracke and Hegner, 1998). This region therefore represents an upper  
630 plate extensional setting, contemporaneously with tearing of the subducting Solomon Sea  
631 slab (Fig. 8c; Holm et al., 2013). The reasons for development of the slab tear are not  
632 understood, but tears in the subducting slab such as this are interpreted to promote increased  
633 fluid flux and metal transport within the mantle, resulting from a larger exposure of the  
634 subducting slab to the surrounding asthenospheric mantle (Richards and Holm, 2013). From  
635 this setting it cannot be conclusively determined which of the two settings, upper plate  
636 extension, or tearing of the subducted slab, contribute more to potential formation of mineral  
637 deposits. However, correlation in the location of the Ladolam deposit above the interpreted  
638 slab tear at the time of formation suggests that it was a combination of the two factors that  
639 likely contributed to mineralization.

640  
641 In the Bismarck Sea, the Solwara deposits of the eastern Bismarck Sea region lie along the  
642 Bismarck Sea fault, a transtensional structure that accommodated sinistral motion between  
643 the North and South Bismarck microplates as well as opening of the Manus Basin (Figs. 1  
644 and 8c; Taylor, 1979; Martinez and Taylor, 1996; Holm et al., 2016). This setting is similar to  
645 that of the Tabar-Lihir-Tanga-Feni island arc chain outlined above, where occurrence of a  
646 dilational upper plate structure likely acted as a preferential conduit that promoted

647 subduction-related magma flux (Figs. 8c). This example emphasizes the important role of  
648 upper plate extension in localizing deposit formation. Preservation is also a major factor for  
649 the Solwara seafloor massive sulfide deposit, where the high-grade, small tonnage nature of  
650 the deposit type is susceptible to erosion or burial beneath younger sediments.

651

## 652 **8. Discussion**

653

654 Mineral deposit exploration methodology is currently undergoing new developments driven  
655 by large databases and advances in technological capabilities (e.g. Cawood and  
656 Hawkesworth, 2015; Butterworth et al., 2016). Such models provide a useful regional context  
657 for deposit formation and an understanding of the large-scale conditions under which deposits  
658 are likely to form. However, at a smaller scale there are always exceptions to these conditions  
659 that arise from dynamic geological settings. For example, in the southwest Pacific and  
660 Southeast Asia episodes of continental accretion took place throughout the Cenozoic  
661 (Audley-Charles, 1981; Petterson et al., 1999; Hill and Hall, 2003; Holm et al., 2013; Holm  
662 et al., 2015b), and microplate tectonics has been active at ever smaller scales (Wallace et al.,  
663 2004; Holm et al., 2016). Through combining our knowledge of plate boundary-scale  
664 processes with inherent regional- and district-scale aberrations in these Earth systems we can  
665 advance our understanding of metallogenesis and achieve greater success in mineral  
666 exploration.

667

668 Comparison of the location, timing, metal content and the frequency of mineral deposit  
669 formation/occurrence with episodes of tectonic reorganization (Fig. 9) reveals a strong  
670 correlation. Melanesian arc metallogenesis (ca. 24-20 Ma), related to collision of the Ontong  
671 Java Plateau and cessation of subduction at the Melanesian trench, was a Cu-rich but

672 relatively minor event in terms of total known metal endowment. In contrast, the overprinting  
673 West Bismarck, New Britain and Solomon arcs host Cu-Au mineral deposits that formed  
674 during a distinct metallogenic episode from ca. 6 Ma and became decisively Au-rich from ca.  
675 3 Ma (Fig. 9). This may represent a major episode of intrusive activity and metal-endowment  
676 within the region, which was linked to the onset of regional microplate tectonics from ca. 6  
677 Ma. Correlation of the New Guinea Orogen metallogenesis with regional tectonics reveals  
678 two discrete episodes of deposit formation related to different tectonic events. The first  
679 deposit-forming event related to Australian continental collision, waning medium-K calc-  
680 alkaline Maramuni arc magmatism and orogenesis from ca. 12 Ma up to 6 Ma has a large  
681 copper-rich mineral endowment but few known deposits (Fig. 9). The later deposit-forming  
682 event from ca. 6 Ma may have occurred in response to crustal delamination. It is  
683 characterized by a large number of known deposits related to high-K calc-alkaline to  
684 shoshonitic (and minor intra-plate alkalic) magmatism, but these represent a smaller  
685 endowment in comparison to the 12-6 Ma event, with no clear preference in commodity.  
686 There is no correlation between the composition of the magmatism and occurrences of  
687 mineralization with a broad compositional spectrum from medium-K calc-alkaline through to  
688 shoshonitic intrusives and even intra-plate alkalic compositions related to deposits in the New  
689 Guinea Orogen and Papuan Peninsula; adakitic compositions, however, are commonly linked  
690 to mineral deposits throughout the islands of eastern Papua New Guinea and the Solomon  
691 Islands. Importantly, formation of deposits does occur over narrow time intervals that suggest  
692 association with regional and discrete tectonic events, such as those interpreted to occur in  
693 association with subduction at the Pocklington trough.

694

695 An evaluation of the nature and variability of the diverse geodynamic settings for deposit  
696 emplacement through time, and the relationship with the southwest Pacific magmatic arcs

697 and associated subduction dynamics, can provide crucial insights into the array of deposit  
698 settings at ancient convergent margins. For example, given current plate motion and  
699 convergence rates, it is expected that the Ontong Java Plateau will collide with the Australian  
700 continent in approximately 20 million years, resulting in a vast orogen along northeast  
701 Australia. The orogen will comprise accreted and highly strained terranes that include the  
702 island arcs of eastern Papua New Guinea and the Solomon Islands, and the already composite  
703 terranes of mainland Papua New Guinea. In this orogen, the different episodes of mineral  
704 deposit formation described above will likely be superimposed on one another. This  
705 underscores the importance of recognizing different terranes and tectonic complications in  
706 present-day convergent margins, such as the southwest Pacific, to successfully unravel  
707 ancient collisional margins such as the North American Cordillera (e.g. Sillitoe, 2008) or the  
708 Tasmanides of eastern Australia (e.g. Cooke et al., 2007; Glen et al., 2007). This study  
709 provides a benchmark for our understanding of the tectonic evolution and metallogensis of  
710 Papua New Guinea and the Solomon Islands, and an analogue with which to compare  
711 complex convergent margins globally. By developing such an understanding of the intricacies  
712 and aberrations that exist within convergent margin tectonics we can further develop and  
713 refine regional exploration models.

714

## 715 **9. Conclusions**

716

717 A strong correlation between deposit formation and episodes of tectonic reorganization is  
718 interpreted for the Papua New Guinea and the Solomon Islands region. The first metallogenic  
719 event is result of collision of the Ontong Java Plateau with the Solomon Islands at ca. 26 Ma  
720 and correlates with formation of copper-rich mineral deposits throughout the Melanesian arc  
721 between ca. 24 and 20 Ma. Subsequent collision of the Australian continent with Papua New

722 Guinea at ca. 12 Ma resulted in two discernible metallogenic events: 1) formation of ca. 12-6  
723 Ma copper-rich mineral deposits associated with medium-K to high-K calc-alkaline  
724 magmatism and development of the New Guinea Orogen, and 2) formation of ca. 6-0 Ma  
725 gold and copper mineral deposits related to delamination of the stagnated slab following  
726 collision, and genetically linked to diverse high-K calc-alkaline and alkaline magmatic  
727 compositions. The emergence of microplate tectonics in eastern Papua New Guinea and the  
728 Solomon Islands from ca. 6 Ma resulted in highly dynamic and discrete kinematic settings  
729 throughout the region. Prospective settings for gold-rich deposit formation are interpreted to  
730 be related to the localization of mineralized corridors above tearing of a subducted slab and  
731 development of slab windows, or upper plate structures related to extension or shortening that  
732 promote magma-flux from the underlying mantle and act as an upper plate conduit for fluid-  
733 flow (e.g., eastern Bismarck Sea Fault). These findings suggest that a good understanding of  
734 geodynamic settings through time, both on the scale of regional subduction zones and  
735 district-scale structure, have the potential to contribute to prospectivity studies and the  
736 generation of new exploration targets at regional scales.

737

### 738 **Acknowledgments**

739

740 R. Holm thanks Simon Richards, Carl Spandler and Yi Hu for fruitful discussions and  
741 analytical assistance, and also J. Espi, Petromin PNG and Barrick Australia for support. S.  
742 Tapster thanks British Geological Survey University Funding Initiative PhD studentship  
743 (S176), NIGFSC (IP-1212-1110), and SEG Newmont Student Research grant (2274). This  
744 work could not have been possible without support provided by the Solomon Island  
745 Geological Survey and Ministry of Mines, Newmont Mining, SolGold (A.R.M) and the team  
746 of Allied Gold. Nick Roberts and Vanessa Pashley of NIGL are thanked for their analytical

747 assistance. Robert Hall, Peter Holling, Georges Beaudoin and an anonymous reviewer are  
748 thanked for their comments and feedback on previous versions of this manuscript;  
749 anonymous reviewers and Franco Pirajno are also thanked for constructive reviews and  
750 editorial assistance on the manuscript.

751

## 752 **References**

753

754 Abbott, L.D., 1995. Neogene tectonic reconstruction of the Adelbert-Finisterre-New Britain  
755 collision, northern Papua New Guinea. *Journal of Southeast Asian Earth Sciences*, 11, 33–51.

756

757 Abbott, L.D., Silver, E.A., Galewsky, J., 1994. Structural evolution of a modern arc–  
758 continent collision in Papua New Guinea. *Tectonics*, 13, 1007–1034.

759

760 Abers, G.A., Ferris, A., Craig, M., Davies, H., Lerner-Lam, A.L., Mutter, J.C., Taylor, B.,  
761 2002. Mantle compensation of active metamorphic core complexes at Woodlark rift in Papua  
762 New Guinea. *Nature*, 418, 862-865.

763

764 Adshead, N.D., 1997. The setting and characteristics of the Umuna epithermal gold-silver  
765 deposit, Misima Island, Papua New Guinea. In: Hancock, G., 1997. *Proceedings of the*  
766 *Geology, Exploration and Mining Conference, Madang*. Australasian Institute of Mining and  
767 *Metallurgy, Parkville*, 1–7.

768

769 Amante, C. and B.W. Eakins, 2009. ETOPO1 1 Arc-Minute Global Relief Model:  
770 *Procedures, Data Sources and Analysis*. NOAA Technical Memorandum NESDIS NGDC-24.  
771 National Geophysical Data Center, NOAA.



772

773 Arnold, G.O., Griffin, T.J., 1978. Intrusions and porphyry copper prospects of the Star  
774 Mountains, Papua New Guinea. In: Gustafson, L.B., and Titley, S.R., eds. Porphyry copper  
775 deposits of the southwestern Pacific islands and Australia, *Economic Geology*, 73, 785-795.

776

777 Ashley, P.M., Flood, R.H., 1981. Low- K tholeiites and high- K igneous rocks from  
778 Woodlark Island, Papua New Guinea. *Journal of the Geological Society of Australia*, 28,  
779 227-240.

780

781 Audley-Charles, M.G., 1981. Geometrical problems and implications of large scale  
782 overthrusting in the Banda Arc–Australian margin collision zone. In: McClay, K.R.  
783 (Ed.), *Thrust and Nappe Tectonics: Geological Society of London Special Publication 9*,  
784 407–416.

785

786 Baldwin, S.L., Fitzgerald, P.G., Webb, L.E., 2012. Tectonics of the New Guinea Region.  
787 *Annual Review of Earth and Planetary Sciences*, 40, 495–520.

788

789 Benes, V., Scott, S.D., Binns, R.A., 1994. Tectonics of rift propagation into a continental  
790 margin: Western Woodlark Basin, Papua New Guinea. *Journal of Geophysical Research*, 99,  
791 4439-4455.

792

793 Boyden, J.A., Müller, R.D., Gurnis, M., Torsvik, T.H., Clark, J.A., Turner, M., Ivey-Law, H.,  
794 Watson, R.J., Cannon, J.S., 2011. Next-generation plate-tectonic reconstructions using  
795 GPlates. In: Keller, G.R., Baru, C. (Eds.), *Geoinformatics: Cyberinfrastructure for the Solid*  
796 *Earth Sciences*. Cambridge University Press, 95-114.

797

798 Bradshaw, M., 1992. South West Pacific Data Package, BMR-APIRA Phanerozoic History of  
799 Australia Project. Record 1992/41, Palaeogeography 43. Bureau of Mineral Resources,  
800 Geology and Geophysics, and the Petroleum Division of the Australian Mineral Industry  
801 Research Association.

802

803 Burkett, D., Graham, I., Spencer, L., Lennox, P., Cohen, D., Zwingmann, H., Lau, F., Kelly,  
804 B., Cendon, D., 2015. The Kulumadau epithermal breccia-hosted gold deposit, Woodlark  
805 Island, Papua New Guinea. Proceeding PACRIM Congress, Hong Kong, China.

806

807 Butterworth, N., Steinberg, D., Müller, R.D., Williams, S., Merdith, A.S., Hardy, S., 2016.  
808 Tectonic environments of South American porphyry copper magmatism through time  
809 revealed by spatiotemporal data mining. *Tectonics*, 35, 2847–2862.

810

811 Carswell, J.T., 1990. Wau gold deposits. Australasian Institute of Mining and Metallurgy  
812 Monograph Series, 14, 1763-1767.

813

814 Cawood, P.A., Hawkesworth, C.J., 2015. Temporal relations between mineral deposits and  
815 global tectonic cycles. In: Jenkin, G.R.T., Lusty, P.A.J., McDonald, I., Smith, M.P., Boyce,  
816 A.J., Wilkinson, J.J. (eds) 2015. *Ore Deposits in an Evolving Earth*. Geological Society,  
817 London, Special Publications, 393, 9–21.

818

819 Chadwick, J., Perfit, M., McInnes, B., Kamenov, G., Plank, T., Jonasson, I., Chadwick, C.,  
820 2009. Arc lavas on both sides of a trench: Slab window effects at the Solomon Islands triple  
821 junction, SW Pacific. *Earth and Planetary Science Letters*, 279, 293–302.

822

823 Chapple, K.G., Ibil, S., 1998. Gameta gold deposit. Australasian Institute of Mining and  
824 Metallurgy Monograph Series, 22, 849-854.

825

826 Chiaradia, M., 2009. Adakite-like magmas from fractional crystallization and melting-  
827 assimilation of mafic lower crust (Eocene Macuchi arc, Western Cordillera, Ecuador).  
828 Chemical Geology, 265, 468–487.

829

830 Chiaradia, M., Müntener, O., Beate, B., Fontignie, D., 2009. Adakite-like volcanism of  
831 Ecuador: Lower crust magmatic evolution and recycling. Contributions to Mineralogy and  
832 Petrology, 158, 563–588.

833

834 Chivas, A.R., and McDougall, I., 1978. Geochronology of Koloula-Porphyry-Copper-  
835 Prospect, Guadalcanal, Solomon-Islands. Economic Geology, 73, 678–689.

836

837 Cloos, M., Sapiie, B., van Ufford, A.Q., Weiland, R.J., Warren, P.Q., McMahon, T.P., 2005.  
838 Collisional delamination in New Guinea: The geotectonics of subducting slab breakoff.  
839 Geological Society of America, Special Paper, 400.

840

841 Cooke, D.R., Hollings, P., Walshe, J.L., 2005. Giant porphyry deposits: Characteristics,  
842 distribution, and tectonic controls. Economic Geology, 100, 801-818.

843

844 Cooke, R.A., Wilson, A.J., House, M.J., Wolfe, R.C., Walshe, J.L., Lickford, V., Crawford,  
845 A.J., 2007. Alkalic porphyry Au-Cu and associated mineral deposits of the Ordovician to

- 846 Early Silurian Macquarie Arc, New South Wales. *Australian Journal of Earth Sciences*, 54,  
847 445-463.
- 848
- 849 Cooper, P., Taylor, B., 1987. Seismotectonics of New Guinea: a model for arc reversal  
850 following arc-continent collision. *Tectonics*, 6, 53–67.
- 851
- 852 Corbett, G.J. and Leach, T.M., 1998. Southwest Pacific rim gold-copper systems: structure,  
853 alteration, and mineralization (p. 234). Society of Economic Geologists.
- 854
- 855 Cowley, S., Mann, P., Coffin, M.F., Shipley, T.H., 2004. Oligocene to Recent tectonic history  
856 of the Central Solomon intra-arc basin as determined from marine seismic reflection data and  
857 compilation of onland geology. *Tectonophysics*, 389, 267–307.
- 858
- 859 Craig, M.S., Warvakai, K., 2009. Structure of an active foreland fold and thrust belt, Papua  
860 New Guinea. *Australian Journal of Earth Sciences*, 56, 719–738.
- 861
- 862 Crowhurst, P.V., Hill, K.C., Foster, D.A., Bennett, A.P., 1996. Thermochronological and  
863 geochemical constraints on the tectonic evolution of northern Papua New Guinea. *Geological*  
864 *Society, London, Special Publications*, 106, 525–537.
- 865
- 866 Crowhurst, P.V., Maas, R., Hill, K.C., Foster, D.A., Fanning, C.M., 2004. Isotopic  
867 constraints on crustal architecture and Permo-Triassic tectonics in New Guinea: possible  
868 links with eastern Australia. *Australian Journal of Earth Sciences*, 51, 107–122.
- 869
- 870 Davey, F.J., 1982. The structure of the South Fiji Basin. *Tectonophysics*, 87, 185–241.

871

872 Davies, H.L., 1990. Structure and evolution of the border region of New Guinea. In: Carman,  
873 G.J., Carman, Z. (Eds.), Petroleum exploration in Papua New Guinea. Proceedings of the  
874 First PNG Petroleum Convention. PNG Chamber of Mines and Petroleum, Port Moresby, pp.  
875 245-269.

876

877 Davies, H.L., 2012. The geology of New Guinea – the cordilleran margin of the Australian  
878 continent. Episodes, 35, 87–102.

879

880 Davies, H.L., Lock, J., Tiffin, D.L., Honza, E., Okuda, Y., Murakami, F., Kisimoto, K., 1987.  
881 Convergent tectonics in the Huon Peninsula region, Papua New Guinea. Geo-Marine Letters  
882 7, 143–152.

883

884 DeMets, C., Gordon, R.G., Argus, D.F., 2010. Geologically current plate motions.  
885 Geophysical Journal International, 181, 1-80.

886

887 Denham, D., 1969. Distribution of Earthquakes in the New Guinea–Solomon Islands region.  
888 Journal of Geophysical Research, 74, 4290–4299.

889

890 Dow, D.B., 1977. A geological synthesis of Papua New Guinea. Bureau of Mineral  
891 Resources, Geology and Geophysics 201, 41pp.

892

893 Dow, D.B., Smit, J.A.J., Bain, J.H.C., Ryburn, R.J., 1972. Geology of the South Sepik  
894 Region, New Guinea. Bureau of Mineral Resources, Geology and Geophysics 133, 87pp.

895

896 Dugmore, M.A., Leaman, P.W., 1998. Mount Bini copper-gold deposit. Australasian Institute  
897 of Mining and Metallurgy Monograph Series, 22, 843-848.

898

899 Dunkley, P.N., 1986. Geology of the New Georgia Group, Solomon Islands. British  
900 Geological Survey Overseas Directorate, British Technical Cooperation Project, Western  
901 Solomon Islands Geological Mapping Project (21).

902

903 Findlay, R.H., 2003. Collision tectonics of northern Papua New Guinea: key field  
904 relationships demand a new model. In: Hillis, R.R., Müller, R.D. (Eds.), Evolution and  
905 Dynamics of the Australian Plate. Geological Society of Australia Special Publication 22 and  
906 Geological Society of America Special Paper 372, Pp. 291–308.

907

908 Gaina, C., Müller, D., 2007. Cenozoic tectonic and depth/age evolution of the Indonesian  
909 gateway and associated back-arc basins. Earth-Science Reviews, 83, 177–203.

910

911 Garwin, S., Hall, R., Watanabe, Y., 2005. Tectonic setting, geology, and gold and copper  
912 mineralization in Cenozoic magmatic arcs of Southeast Asia and the west Pacific. Economic  
913 Geology 100<sup>th</sup> Anniversary Volume, 891-930.

914

915 Glen, R.A., Crawford, A.J., Cooke, D.R., 2007. Tectonic setting of porphyry Cu-Au  
916 mineralization in the Ordovician-Early Silurian Macquarie Arc, Eastern Lachlan Orogen,  
917 New South Wales. Australian Journal of Earth Sciences, 54, 465-479.

918

- 919 Gow, P.A., Walshe, J.L., 2005. The role of preexisting geologic architecture in the formation  
920 of giant porphyry-related Cu ± Au deposits: Examples from New Guinea and Chile.  
921 *Economic Geology*, 100, 819-833.
- 922
- 923 Hackman, B.D., 1980. The geology of Guadalcanal, Solomon Islands. Overseas memoirs HM  
924 Stationery Office, 6, 1-115.
- 925
- 926 Hall, R., 2002. Cenozoic geological and plate tectonic evolution of SE Asia and the SW  
927 Pacific: computer-based reconstructions, model and animations. *Journal of Asian Earth*  
928 *Sciences*, 20, 353-431.
- 929
- 930 Hall, R., Spakman, W., 2002. Subducted slabs beneath the eastern Indonesia-Tonga region:  
931 insights from tomography. *Earth and Planetary Science Letters*, 201, 321-336.
- 932
- 933 Hall, R.J., Britten, R.M., Henry, D.D., 1990. Frieda River copper-gold deposits. *Australasian*  
934 *Institute of Mining and Metallurgy Minigraph Series*, 14, 1709-1715.
- 935
- 936 Hill, K.C., Gleadow, A.J.W., 1989. Uplift and thermal history of the Papuan Fold Belt, Papua  
937 New Guinea: Apatite fission track analysis. *Australian Journal of Earth Sciences*, 36, 515-  
938 539.
- 939
- 940 Hill, K.C., Hall, R., 2003. Mesozoic-Cenozoic evolution of Australia's New Guinea margin  
941 in a west Pacific context. In: Hillis R.R., Müller, R.D. (Eds.) *Evolution and Dynamics of the*  
942 *Australian Plate: Geological Society of Australia Special Publication 22*, and *Geological*  
943 *Society of America Special Paper*, 372, 265-290.

944

945 Hill, K.C., Kendrick, R.D., Crowhurst, P.V., Gow, P.A., 2002. Copper-gold mineralisation in  
946 New Guinea: tectonics, lineaments, thermochronology and structure. *Australian Journal of*  
947 *Earth Sciences*, 49, 737–752.

948

949 Hill, K.C., Raza, A., 1999. Arc–continent collision in Papua Guinea: Constraints from fission  
950 track thermochronology. *Tectonics*, 18, 950–966.

951

952 Hine, R., Bye, S.M., Cook, F.W., Leckie, J.F., Torr, G.L., 1978. The Esis porphyry copper  
953 deposit, East New Britain, Papua New Guinea. *Economic Geology*, 73, 761-767.

954

955 Holm, R.J., Poke, B., 2018. Petrology and crustal inheritance of the Cloudy Bay Volcanics as  
956 derived from a fluvial conglomerate, Papuan Peninsula (Papua New Guinea): An example of  
957 geological inquiry in the absence of in situ outcrop. *Cogent Geoscience*, 4: 1450198.

958

959 Holm, R.J., Richards, S.W., 2013. A re-evaluation of arc-continent collision and along-arc  
960 variation in the Bismarck Sea region, Papua New Guinea. *Australian Journal of Earth*  
961 *Sciences*, 60, 605–619.

962

963 Holm, R.J., Rosenbaum, G., Richards, S.W., 2016. Post 8 Ma reconstruction of Papua New  
964 Guinea and Solomon Islands: Microplate tectonics in a convergent plate boundary setting.  
965 *Earth-Science Reviews*, 156, 66-81.

966



- 967 Holm, R.J., Spandler, C., Richards, S.W., 2013. Melanesian arc far-field response to collision  
968 of the Ontong Java Plateau: Geochronology and petrogenesis of the Simuku Igneous  
969 Complex, New Britain, Papua New Guinea. *Tectonophysics*, 603, 189–212.  
970
- 971 Holm, R.J., Richards, S.W., Rosenbaum, G., Spandler, C., 2015a. Disparate tectonic settings  
972 for mineralisation in an active arc, eastern Papua New Guinea and the Solomon Islands.  
973 Proceedings of PACRIM 2015 Congress, Hong Kong, China.  
974
- 975 Holm, R.J., Spandler, C., Richards, S.W., 2015b. Continental collision, orogenesis and arc  
976 magmatism of the Miocene Maramuni arc, Papua New Guinea. *Gondwana Research*, 28,  
977 1117-1136.  
978
- 979 Hutchison, D.S., Norvick, M.S., 1980. Geology of the North Sepik Region, Papua New  
980 Guinea. Bureau of Mineral Resources, Geology and Geophysics 1980/24, 67pp.  
981
- 982 Hutton, M.J., Akiro, A.K., Cannard, C.J., Syka, M.C., 1990. Kerimenge gold prospect.  
983 Australasian Institute of Mining and Metallurgy Monograph Series, 24, 1769-1772.  
984
- 985 Johnson, R.W., Jaques, A.L., 1980. Continent-arc collision and reversal of arc polarity: New  
986 interpretations from a critical area. *Tectonophysics*, 63, 111-124.  
987
- 988 Johnson, R.W., Mackenzie, D.E., Smith, I.E.M., 1978. Delayed partial melting of subduction-  
989 modified mantle in Papua New Guinea. *Tectonophysics*, 46, 197-216.  
990

- 991 Kay, S.M., Mpodozis, C., 2001. Central Andean ore deposits linked to evolving shallow  
992 subduction systems and thickening crust. *GSA Today*, 11, 4-9.  
993
- 994 Knesel, K.M., Cohen, B.E., Vasconcelos, P.M., Thiede, D.S., 2008. Rapid change in drift of  
995 the Australian plate records collision with Ontong Java plateau. *Nature*, 454, 754–757.  
996
- 997 Kroenke, L.W., 1984. Cenozoic tectonic development of the southwest Pacific. U.N. ESCAP,  
998 CCOP/SOPAC Tech. Bull. 6.  
999
- 1000 Langmead, R.P., McLeod, R.L., 1990. Tolukuma gold deposit. *Australasian Institute of*  
1001 *Mining and Metallurgy*, 14, 1777-1781.  
1002
- 1003 Lindley, I.D., 2006. Extensional and vertical tectonics in the New Guinea islands:  
1004 implications for island arc evolution. Supplement to Scalera, G., Lavecchia, G., *Frontiers in*  
1005 *sciences: new ideas and interpretation. Annals of Geophysics*, 49, 1, 2006.  
1006
- 1007 Lindley, I.D., 1990. Wild Dog gold deposit. *Australasian Institute of Mining and Metallurgy*  
1008 *Monograph Series*, 14, 1789-1792.  
1009
- 1010 Lock, J., Davies, H.L., Tiffin, D.L., Murakami, F., Kisimoto, K., 1987. The Trobriand  
1011 subduction system in the western Solomon Sea. *Geo-Marine Letters* 7, 129–134.  
1012
- 1013 Loucks, R.R., 2014. Distinctive composition of copper-ore-forming arc magmas. *Australian*  
1014 *Journal of Earth Sciences*, 61, 5-16.  
1015

- 1016 Lunge, M., 2013. A mineralogical, geochemical and geochronological study of the Golpu and  
1017 Nambonga North porphyry copper-gold systems, Wafi-Golpu Mineral District, Papua New  
1018 Guinea. Unpublished MSc thesis, University of Papua New Guinea, 156p.  
1019
- 1020 Macpherson, C.G., Dreher, S.T., Thirlwall, M.F., 2006. Adakites without slab melting: High  
1021 pressure differentiation of island arc magma, Mindanao, the Philippines: *Earth and Planetary  
1022 Science Letters*, 243, 581–593.  
1023
- 1024 Mann, P., Taira, A., 2004. Global tectonic significance of the Solomon Islands and Ontong  
1025 Java Plateau convergent zone. *Tectonophysics*, 389, 137–190.  
1026
- 1027 Mann, P., Taylor, F.W., Lagoe, M.B., Quarles, A., Burr, G., 1998. Accelerating late  
1028 Quaternary uplift of the New Georgia Island Group (Solomon island arc) in response to  
1029 subduction of the recently active Woodlark spreading center and Coleman seamount.  
1030 *Tectonophysics*, 295, 259–306.  
1031
- 1032 Martinez, F., Taylor, B., 1996. Backarc spreading, rifting, and microplate rotation, between  
1033 transform faults in the Manus Basin. *Marine Geophysical Research*, 18, 203–224.  
1034
- 1035 McDowell, F.W., McMahon, T.P., Warren, P.Q., Cloos, M., 1996. Pliocene Cu-Au-bearing  
1036 igneous intrusions of the Gunung Bijih (Ertsberg) District, Irian Jaya, Indonesia: K-Ar  
1037 geochronology. *The Journal of Geology*, 104, 327–340.  
1038
- 1039 McInnes, B.I.A., 1992. A glimpse of ephemeral subduction zone processes from Simberi  
1040 Island, Papua New Guinea. Unpublished PhD Thesis, University of Ottawa

1041

1042 McNeil, P.A., 1990. Wapolu gold deposit, Fergusson Island. Australasian Institute of Mining  
1043 and Metallurgy Monograph Series, 14, 1783-1788.

1044

1045 Moyle, A.J., Doyle, B.J., Hoogvliet, H., Ware, A.R., 1990. Ladolam Gold Deposit, Lihir  
1046 Island. In: Geology of the mineral deposits of Australia and Papua New Guinea, Hughes, F.E.  
1047 (Ed), 1793-1805, The Australasian Institute of Mining and Metallurgy, Melbourne. P 1793-  
1048 1805

1049

1050 Müller, R.D., Seton, M., Zahirovic, S., Williams, S.E., Matthews, K.J., Wright, N.W.,  
1051 Shephard, G.E., Maloney, K.T., Barnett-Moore, N., Hosseinpour, M., Bower, D.J., Cannon,  
1052 J., 2016. Ocean basin evolution and global-scale plate reorganization events since Pangea  
1053 breakup. Annual Review of Earth and Planetary Sciences, 44, 107-138.

1054

1055 Nelson, R.W., Bartram, J.A., Christie, M.H., 1990. Hidden Valley gold-silver deposit. In:  
1056 Geology of the mineral deposits of Australia and Papua New Guinea, Hughes, F.E. (Ed),  
1057 1773-1776, The Australasian Institute of Mining and Metallurgy, Melbourne.

1058

1059 Niespolo, E.M., Rutte, D., Deino, A.L. Renne, P.R., 2016. Intercalibration and age of the  
1060 Alder Creek sanidine  $^{40}\text{Ar}/^{39}\text{Ar}$  standard. Quaternary Geochronology.

1061

1062 Ott, B., Mann, P., 2015. Late Miocene to Recent formation of the Aure-Moresby fold-thrust  
1063 belt and foreland basin as a consequence of Woodlark microplate rotation, Papua New  
1064 Guinea. Geochemistry, Geophysics, Geosystems, doi: 10.1002/2014GC005668.

1065

- 1066 Page, R.W., 1976. Geochronology of igneous and metamorphic rocks in the New Guinea  
1067 Highlands. Bureau of Mineral Resources, Geology and Geophysics Bulletin 162, Australian  
1068 Government Publishing Service, Canberra.
- 1069
- 1070 Page, R.W., McDougall, I., 1972a. Geochronology of the Panguna porphyry copper deposit,  
1071 Bougainville Island, New Guinea. *Economic Geology*, 67, 1065-1074.
- 1072
- 1073 Page, R.W., McDougall, I., 1972b. Ages of mineralization of gold and porphyry copper  
1074 deposits in the New Guinea Highlands. *Economic Geology*, 67, 1034-1048.
- 1075
- 1076 Petterson, M.G., Babbs, T., Neal, C.R., Mahoney, J.J., Saunders, A.D., Duncan, R.A., Tolia,  
1077 D., Magu, R., Qopoto, C., Mahoa, H., Natogga, D., 1999. Geological-tectonic framework of  
1078 Solomon Islands, SW Pacific: crustal accretion and growth with an intra-oceanic setting.  
1079 *Tectonophysics*, 301, 35–60.
- 1080
- 1081 Petterson, M.G., Neal, C.R., Mahoney, J.J., Kroenke, L.W., Saunders, A.D., Babbs, T.L.,  
1082 Duncan, R.A., Tolia, D., McGrail, B., 1997. Structure and deformation of north and central  
1083 Malaita, Solomon Islands: tectonic implications for the Ontong Java Plateau-  
1084 Solomon arc collision, and for the fate of oceanic plateaus. *Tectonophysics*, 283, 1–33.
- 1085
- 1086 Phinney, E.J., Mann, P., Coffin, M.F., Shipley, T.H., 2004. Sequence stratigraphy, structural  
1087 style, and age of deformation of the Malaita accretionary prism (Solomon arc-Ontong Java  
1088 Plateau convergent zone). *Tectonophysics*, 389, 221–246.
- 1089

- 1090 Pigram, C.J., Davies, H.L., 1987. Terranes and the accretion history of the New Guinea  
1091 Orogen. *BMR Journal of Australian Geology and Geophysics*, 10, 193–211.  
1092
- 1093 Rapp, R.P., Watson, E.B., 1995. Dehydration melting of metabasalt at 8–32 kbar:  
1094 Implications for continental growth and crust-mantle recycling. *Journal of Petrology*, 36,  
1095 891–931.  
1096
- 1097 Richards, J.P., 2003. Tectono-magmatic precursors for porphyry Cu-(Mo-Au) deposit  
1098 formation. *Economic Geology*, 98, 1515-1533.  
1099
- 1100 Richards, J.P., 2011. High Sr/Y arc magmas and porphyry Cu ± Mo ± Au deposits: Just add  
1101 water. *Economic Geology*, 106, 1075–1081.  
1102
- 1103 Richards, J.P., 2013. Giant ore deposits formed by optimal alignments and combinations of  
1104 geological processes. *Nature Geoscience*, 6, 911-916.  
1105
- 1106 Richards, J.P., Kerrich, R., 2007. Adakite-like rocks: Their diverse origins and questionable  
1107 role in metallogenesis. *Economic Geology*, 102, 537–576.  
1108
- 1109 Richards, J.P., Ledlie, I., 1993. Alkalic intrusive rocks associated with the Mount Kare gold  
1110 deposit, Papua New Guinea; comparison with the Porgera intrusive complex. *Economic*  
1111 *Geology*, 88, 755-781.  
1112

- 1113 Richards, J.P., McDougall, I., 1990. Geochronology of the Porgera gold deposit, Papua New  
1114 Guinea: Resolving the effects of excess argon on K-Ar and  $^{40}\text{Ar}/^{39}\text{Ar}$  age estimates for  
1115 magmatism and mineralization. *Geochimica et Cosmochimica Acta*, 54, 1397-1415.  
1116
- 1117 Richards, S.W., Holm, R.J., 2013. Tectonic preconditioning and the formation of giant  
1118 porphyry deposits. *Economic Geology Special Publication 17*, 265–275.  
1119
- 1120 Rohrbach, A., Schuth, S., Ballhaus, C., Münker, C., Matveev, S., Qopoto, C., 2005.  
1121 Petrological constraints on the origin of arc picrites, New Georgia Group, Solomon Islands.  
1122 *Contributions to Mineralogy and Petrology*, 149, 685-698.  
1123
- 1124 Rosenbaum, G., Giles, D., Saxon, M., Betts, P.G., Weinberg, R.F., Duboz, C., 2005.  
1125 Subduction of the Nazca Ridge and the Inca Plateau: Insights into the formation of ore  
1126 deposits in Peru. *Earth and Planetary Science Letters*, 239, 18-32.  
1127
- 1128 Rosenbaum, G., Mo, W., 2011. Tectonic and magmatic responses to the subduction of high  
1129 bathymetric relief. *Gondwana Research*, 19, 571–582.  
1130
- 1131 Rytuba, J.J., McKee, E.H., Cox, D., 1993. Geochronology and geochemistry of the Ladolam  
1132 gold deposit, Lihir Island, and gold deposits and volcanoes of Tabar and Tatau, Papua New  
1133 Guinea. *USGS Bulletin 2039*, 119-126.  
1134
- 1135 Schellart, W.P., Lister, G.S., Toy, V.G., 2006. A Late Cretaceous and Cenozoic  
1136 reconstruction of the southwest Pacific region: Tectonics controlled by subduction and slab  
1137 rollback processes. *Earth-Science Reviews*, 76, 191-233.

1138

1139 Schellart, W.P., Spakman, W., 2015. Australian plate motion and topography linked to fossil  
1140 New Guinea slab below Lake Eyre. *Earth and Planetary Science Letters*, 421, 107-116.

1141

1142 Schuth, S., Münker, C., König, S., Qopoto, C., Basi, S., Garbe-Schönberg, D., Ballhaus, C.,  
1143 2009. Petrogenesis of lavas along the Solomon Island arc, SW Pacific: Coupling of  
1144 compositional variations and subduction zone geometry. *Journal of Petrology*, 50, 781-811.

1145

1146 Sen, C., Dunn, T., 1994. Dehydration melting of a basaltic composition amphibolite at 1.5  
1147 and 2.0 GPa: Implications for the origin of adakites. *Contributions to Mineralogy and  
1148 Petrology*, 117, 394-409.

1149

1150 Seton, M., Mortimer, N., Williams, S., Quilty, P., Gans, P., Meffre, S., Micklethwaite, S.,  
1151 Zahirovic, S., Moore, J., Matthews, K.J., 2016. Melanesian back-arc basin and arc  
1152 development: Constraints from the eastern Coral Sea. *Gondwana Research*, 39, 77-95.

1153

1154 Seton, M., Müller, R.D., Zahirovic, S., Gaina, C., Torsvik, T., Shephard, G., Talsma, A.,  
1155 Gurnis, M., Turner, M., Maus, S., Chandler, M., 2012. Global continental and ocean basin  
1156 reconstructions since 200 Ma. *Earth-Science Reviews*, 113, 212-270.

1157

1158 Sillitoe, R.H., 1989. Gold deposits in western Pacific island arcs; the magmatic connection.  
1159 *Economic Geology Monograph*, 6, 274-291.

1160



- 1161 Sillitoe, R.H., 2008. Major gold deposits and belts of the North and South American  
1162 Cordillera: Distribution, tectonomagmatic setting, and metallogenic considerations.  
1163 *Economic Geology*, 103, 663-687.  
1164
- 1165 Sillitoe, R.H., 2010. Porphyry copper systems. *Economic Geology*, 105, 3-41.  
1166
- 1167 Singer, D.A., Berger, V.I., Moring, B.C., 2008. Porphyry copper deposits of the world:  
1168 Database and grade and tonnage models. U.S., Geological Survey Open-File Report 2008-  
1169 1155.  
1170
- 1171 Smith, I. E. M., 1976. Volcanic rocks from southeastern Papua: The Evolution of volcanism  
1172 at a plate boundary (Unpublished PhD Thesis, p. 298). Canberra: Australian National  
1173 University.  
1174
- 1175 Smith, I. E., 1982. Volcanic evolution in eastern Papua. *Tectonophysics*, 87, 315-333.  
1176
- 1177 Smith, D.J., Jenkin, G.R.T., Naden, J., Boyce, A.J., Petterson, M.G., Toba, T., Darling, W.G.,  
1178 Taylor, H., Millar, I.L., 2010. Anomalous alkaline sulphate fluids produced in a magmatic  
1179 hydrothermal system—Savo, Solomon Islands. *Chemical Geology*, 275, 35-49.  
1180
- 1181 Smith, D.J., Jenkin, G.R.T., Petterson, M.G., Naden, J., Fielder, S., Toba, T., Chenery,  
1182 S.R.N., 2011. Unusual mixed silica-carbonate deposits from magmatic-hydrothermal hot  
1183 springs, Savo, Solomon Islands. *Journal of the Geological Society*, 168, 1297-1310.  
1184

- 1185 Smith, D., Petterson, M., Saunders, A., Millar, I.L., Jenkin, G.R.T., Toba, T., Naden, J.,  
1186 Cook, J.M., 2009. The petrogenesis of sodic island arc magmas at Savo Volcano, Solomon  
1187 Islands. *Contributions to Mineralogy and Petrology*, 158, 785–801.  
1188
- 1189 Stracke, A., Hegner, E., 1998. Rifting-related volcanism in an oceanic post-collisional  
1190 setting: the Tabar-Lihir-Tanga-Feni (TLTF) island chain, Papua New Guinea. *Lithos*, 45,  
1191 545-560.  
1192
- 1193 Struckmeyer, H.I.M., Yeung, M., Pigram, C.J., 1993. Mesozoic to Cainozoic plate tectonic  
1194 palaeographic evolution of the New Guinea region. In: Carman, G. J., Carman, Z. (Eds.),  
1195 Petroleum Exploration in Papua New Guinea. Proceedings of the Second PNG Petroleum  
1196 Convention, Port Moresby, 261–290.  
1197
- 1198 Swiridiuk, P., 1998. Exploring the Solomon Islands with airborne geophysics. *Exploration*  
1199 *Geophysics*, 29, 620–625  
1200
- 1201 Taira, A., Mann, P., Rahardiawan, R., 2004. Incipient subduction of the Ontong Java Plateau  
1202 along the North Solomon trench. *Tectonophysics*, 389, 247-266.  
1203
- 1204 Tapster, S., Condon, D.J., Naden, J., Noble, S.R., Petterson, M.G., Roberts, N.M.W.,  
1205 Saunders, A.D., Smith, D.J., 2016. Rapid thermal rejuvenation of high-crystallinity magma  
1206 linked to porphyry copper deposit formation; evidence from the Koloula Porphyry Prospect,  
1207 Solomon Islands. *Earth and Planetary Science Letters*, 442, 206-217.  
1208

- 1209 Tapster, S., Petterson., M.G, Jenkin, G.R.T, Saunders., A.,D, Smith, D.J, Naden, J., 2011.  
1210 Preliminary petrogenetic and geodynamic controls on magmatic-hydrothermal Cu and Au  
1211 mineralisation of Guadalcanal, Solomon Islands. In Barra, F. et al. (Eds) LET'S TALK ORE  
1212 DEPOSITS. Proceedings of the 11th Biennial SGA Meeting, Antofagasta, Chile, 2, 577-579.  
1213
- 1214 Tapster, S., Roberts, N.M.W., Petterson, M.G., Saunders, A.D., Naden, J., 2014. From  
1215 continent to intra-oceanic arc: Zircon xenocrysts record the crustal evolution of the Solomon  
1216 island arc. *Geology*, 42, 1087-1090.  
1217
- 1218 Taylor, B., 1979. Bismarck Sea: Evolution of a back-arc basin. *Geology*, 7, 171-174.  
1219
- 1220 Taylor, B., Goodliffe, A.M., Martinez, F., 1999. How continents break up: Insights from  
1221 Papua New Guinea. *Journal of Geophysical Research*, 104, 7497-7512.  
1222
- 1223 Taylor, B., Goodliffe, A., Martinez, F., Hey, R., 1995. Continental rifting and initial sea-floor  
1224 spreading in the Woodlark basin. *Nature*, 374, 534-537.  
1225
- 1226 Thomas, R.J., Spencer, C., Bushi, A.M., Baglow, N., Boniface, N., de Kock, G., Horstwood,  
1227 M.S., Hollick, L., Jacobs, J., Kajara, S. Kamihanda, G., 2016. Geochronology of the central  
1228 Tanzania Craton and its southern and eastern orogenic margins. *Precambrian Research*, 277,  
1229 47-67.  
1230
- 1231 Titley, S.R., 1978. Geologic history, hypogene features, and processes of secondary sulfide  
1232 enrichment at the Plesyumi copper prospect, New Britain, Papua New Guinea. *Economic  
1233 Geology*, 73, 768-784.

1234

1235 Turner, C.C. Ridgway, J., 1982. Tholeiitic, calc-alkaline and (?) alkaline igneous rocks of the  
1236 Shortland islands, Solomon Islands. *Tectonophysics*, 87, 335-354.

1237

1238 Van Donge, M., Weinberg, R.F., Tomkins, A.G., 2010a. REE-Y, Ti, and P remobilization in  
1239 magmatic rocks by hydrothermal alteration during Cu-Au deposit formation. *Economic  
1240 Geology*, 105, 763-776.

1241

1242 van Dongen, M., Weinberg, R.F., Tomkins, A.G., Armstrong, R.A., Woodhead, J.D., 2010b.  
1243 Recycling of Proterozoic crust in Pleistocene juvenile magma and rapid formation of the Ok  
1244 Tedi porphyry Cu-Au deposit, Papua New Guinea. *Lithos*, 114, 282–292.

1245

1246 Wallace, L.M., Ellis, S., Little, T., Tregoning, P., Palmer, N., Rosa, R., Stanaway, R., Oa, J.,  
1247 Nidkombu, E., Kwazi, J., 2014. Continental breakup and UHP rock exhumation in action:  
1248 GPS results from the Woodlark Rift, Papua New Guinea. *Geochemistry, Geophysics,  
1249 Geosystems*, 15, 4267-4290.

1250

1251 Wallace, L.M., Stevens, C., Silver, E., McCaffrey, R., Loratung, W., Hasiata, S., Stanaway,  
1252 R., Curley, R., Rosa, R., Taugaloidi, J., 2004. GPS and seismological constraints on active  
1253 tectonics and arc-continent collision in Papua New Guinea: Implications for mechanics of  
1254 microplate rotations in a plate boundary zone. *Journal of Geophysical Research*, 19, B05404,  
1255 doi:10.1029/2003JB002481.

1256

- 1257 Webb, L.E., Baldwin, S.L., Fitzgerald, P.G., 2014. The Early-Middle Miocene subduction  
1258 complex of the Louisiade Archipelago, southern margin of the Woodlark Rift. *Geochemistry,*  
1259 *Geophysics, Geosystems*, 15, 4024-4046.
- 1260
- 1261 Weiland, R. J., 1999. Emplacement of the Irian Ophiolite and unroofing of the Ruffaer  
1262 Metamorphic Belt of Irian Jaya, Indonesia. PhD thesis, University of Texas at Austin, 526 pp.
- 1263
- 1264 Wells, R.E., 1989. Origin of the oceanic basalt basement of the Solomon Islands arc and its  
1265 relationship to the Ontong Java Plateau – insights from Cenozoic plate motion models.  
1266 *Tectonophysics*, 165, 219–235.
- 1267
- 1268 Whalen, J.B., Britten, R.M., McDougall, I., 1982. Geochronology and geochemistry of the  
1269 Frieda River prospect area, Papua New Guinea. *Economic Geology*, 77, 592-616.
- 1270
- 1271 Wilcox, R.E., Harding, T.P., Seely, D.R., 1973. Basic wrench tectonics. *American*  
1272 *Association of Petroleum Geologists*, 57, 74–96.
- 1273
- 1274 Woodhead, J.D., Eggins, S.M., Johnson, R.W., 1998. Magma genesis in the New Britain  
1275 island arc: Further insights into melting and mass transfer processes. *Journal of Petrology*, 39,  
1276 1641-1668.
- 1277
- 1278 Woodhead, J., Hergt, J., Sandiford, M., Johnson, W., 2010. The big crunch: Physical and  
1279 chemical expressions of arc/continent collision in the Western Bismarck arc. *Journal of*  
1280 *Volcanology and Geothermal Research*, 190, 11–24.
- 1281

**Figure Captions**

1282

1283

1284 **Figure 1.** Mineral deposits of the Papua New Guinea and Solomon Islands region. Red points  
1285 indicate deposits and prospects host to samples dated in this study.

1286

1287 **Figure 2.** Tectonic setting of Papua New Guinea and Solomon Islands. A) Regional plate  
1288 boundaries and tectonic elements. Light grey shading illustrates bathymetry <2000 m below  
1289 sea level indicative of continental or arc crust, and oceanic plateaus. The New Guinea Orogen  
1290 comprises rocks of the New Guinea Mobile Belt and the Papuan Fold and Thrust Belt;  
1291 Adelbert Terrane (AT); Aure-Moresby trough (AMT); Bougainville Island (B); Bismarck Sea  
1292 fault (BSF); Bundi fault zone (BFZ); Choiseul Island (C); Feni Deep (FD); Finisterre Terrane  
1293 (FT); Guadalcanal Island (G); Gazelle Peninsula (GP); Kia-Kaipito-Korigole fault zone  
1294 (KKKF); Lagaip fault zone (LFZ); Malaita Island (M); Manus Island (MI); New Britain  
1295 (NB); New Georgia Islands (NG); New Guinea Mobile Belt (NGMB); New Ireland (NI);  
1296 Papuan Fold and Thrust Belt (PFTB); Ramu-Markham fault (RMF); Santa Isabel Island (SI);  
1297 Sepik arc (SA); Weitin Fault (WF); West Bismarck fault (WBF); Willaumez-Manus Rise  
1298 (WMR). Arrows indicate rate and direction of plate motion of the Australian and Pacific  
1299 plates (MORVEL, DeMets et al., 2010); B) Pliocene-Quaternary volcanic centres and  
1300 magmatic arcs related to this study. Figure modified from Holm et al. (2016). Subduction  
1301 zone symbols with filled pattern denote active subduction; empty symbols denote extinct  
1302 subduction zone or negligible convergence.

1303

1304 **Figure 3.** Grade vs tonnage plots for A) gold and B) copper for mines, deposits and prospects  
1305 with reported resources. Note logarithmic scale for metal grades and tonnage; data are listed  
1306 in Table 1.

1307

1308 **Figure 4.** U-Pb dating results for A) Ipi River 109472a; B) Baia JD15; C) Tirua Hill SI1059;  
1309 D) Fauro Island SI11886; and E) Sutakiki SK001346.

1310

1311 **Figure 5.** Ar-Ar dating results for Gold Ridge samples GDC5 45.8m and GDC3 279.45m.

1312

1313 **Figure 6.** Tectonic reconstruction for collision of the Ontong Java Plateau with the  
1314 Melanesian arc and deposit formation for 30 Ma and 26-20 Ma. Green regions denote the  
1315 present-day landmass using modern coastlines; grey regions are indicative of crustal extent  
1316 using the 2000 m bathymetric contour. The reconstruction is presented here without a specific  
1317 reference frame for ease of visualization, please see the reconstruction files in the  
1318 supplementary material for specific reference frames.

1319

1320 **Figure 7.** Tectonic reconstruction for the period 20-0 Ma, illustrating collision of the  
1321 Australian continent with the New Guinea Mobile Belt versus the Hall (2002) reconstruction  
1322 model of Trobriand trough subduction. Syn-orogenic deposit formation from 12-6 Ma, and  
1323 post-orogenic formation from 6-0 Ma are shown for correlation. Green regions denote the  
1324 present-day landmass using modern coastlines; grey regions are indicative of crustal extent  
1325 using the 2000 m bathymetric contour. The reconstruction is presented here relative to a fixed  
1326 Australia reference frame for ease of visualization, please see the reconstruction files in the  
1327 supplementary material for specific reference frames.

1328

1329 **Figure 8.** Selected tectonic reconstructions and mineral deposit formation for key areas and  
1330 times within the eastern Papua New Guinea and Solomon Islands region. A) Formation of the

1331 Panguna and Fauro Island Deposits above the interpreted subducted margin of the Solomon  
1332 Sea plate-Woodlark Basin, and Mase deposit above the subducting Woodlark spreading  
1333 center; B) Formation of the New Georgia deposits above the subducting Woodlark spreading  
1334 center, and Guadalcanal deposits above the subducting margin of the Woodlark Basin; C)  
1335 Formation of the Solwara deposits related to transtension along the Bismarck Sea fault above  
1336 the subducting Solomon Sea plate, and deposits of the Tabar-Lihir-Tanga-Feni island arc  
1337 chain related to upper plate extension (normal faulting indicated by hatched linework  
1338 between New Ireland and Bougainville), while the Ladolam deposit forms above a tear in the  
1339 subducting slab. Interpreted Solomon Sea slab (light blue shaded area for present-day) is  
1340 from Holm and Richards (2013); the reconstructed surface extent or indicative trend of slab  
1341 structure is indicated by the dashed red lines. Green regions denote the present-day landmass  
1342 using modern coastlines; grey regions are indicative of crustal extent using the 2000 m  
1343 bathymetric contour. The reconstruction is presented here relative to the global moving  
1344 hotspot reference frame, please see the reconstruction files in the supplementary material for  
1345 specific reference frames.

1346

1347 **Figure 9.** Mineral endowment for Papua New Guinea and Solomon Islands through time.  
1348 Total contained Cu and Au tonnage are shown at time of deposit formation, with number of  
1349 deposits in 3 Myr bins. Deposits are differentiated into the island arc terranes for the  
1350 Melanesian, West Bismarck, New Britain and Solomon arcs, and the New Guinea Orogen  
1351 with deposits related to the Maramuni arc.

1352



1354 **Tectonic evolution and copper-gold metallogensis of the Papua New**  
1355 **Guinea and Solomon Islands region**

1356

1357 Robert J. Holm, Simon Tapster, Hielke A. Jelsma, Gideon Rosenbaum, Darren F. Mark

1358

1359

1360 • We provide a new model that explains the timing and location for deposit formation.

1361 • Deposit formation is linked to collision events and onset of microplate tectonics.

1362 • Six new ages for mineral deposits are provided.

1363 • A comprehensive database of mines, deposits and prospects is included.

1364

1365